CHAPTER 3

Results

3.1 Screening of total phenolic and flavonoid contents, antioxidant and antiglycation activities of culinary plants

This study involved twenty six culinary plants that are regularly consumed and applied in traditional medicines in Thailand. The extracts obtained by sequential solvent extractions, such as ethyl acetate (EA) and ethanol, were screened for their total phenolic and flavonoid contents, antiodixant activity based on DPPH radical scavenging assay and antiglycation activity in BSA-glucose model system.

3.1.1 Total phenolic and flavonoid contents

The phenolic content was determined by the Folin-Ciocalteu method and expressed as mg gallic acid equivalent (GAE) per gram of dry sample. Table 3.1 shows the content of phenolic compounds in various plant extracts ranging from 0.02 to 3.13 mg/g sample. High amounts of phenolic compounds were significantly ($p < 0.05$) found in ethanolic (ET) fractions of *P. granatum* (3.13 mg/g), *D. longan* (1.68 mg/g), *M. indica* (1.51 mg/g) and the ethyl acetate (EA) fractions of *D. longan* (1.20 mg/g) and *P. granatum* (1.11 mg/g), respectively. The total flavonoid content in each plant extract was also determined using a colorimetric method and reported as the μg quercetin equivalent (QE) per gram of dried sample. The results showed that the content of the flavonoid ranged from 0.0014 to 0.24 mg/g (Table 3.1). The significantly highest amount of flavonoids ($p < 0.05$) was shown in the ET fraction of *P. granatum* (0.24 mg/g) followed by *D. longan* (0.16 mg/g), *M. indica* (0.15 mg/g) and the EA fraction of

Table 3.1 Total phenolic and total flavonoid contents in the ethyl acetate (EA) and ethanolic (ET) extracts of the culinary plants

Plants	Total phenolic content (mg GAE/g extract)		Total flavonoid content (mg QE/g extract)	
	EA extract	ET extract	EA extract	ET extract
1. Spices and condiments (9 species)				
M. cordifolia Opiz.	0.20±0.0	0.16±0.0	0.08±0.0	0.06±0.0
O. sanctum (green)	0.20±0.0	0.26±0.0	0.04±0.0	0.06±0.0
P. odoratum	0.28±0.0	0.38±0.1	0.07±0.0	0.08±0.0
P. sarmentosum	0.10±0.0	0.32±0.0	0.05±0.0	0.10±0.0^{d}
A. galangal	0.08±0.0	0.07±0.0	0.02±0.0	0.002±0.0
Z. officinale Rose.	0.06±0.0	0.08±0.0	0.02±0.0	0.01±0.0
A. cepa	0.04±0.0	0.04±0.0	0.003±0.0	0.008±0.0
A. ascalonicum	0.04±0.0	0.10±0.0	0.004±0.0	0.006±0.0
A. sativum	ND	0.02±0.0	0.003±0.0	0.001±0.0
2. Vegetables (9 species)				
L. leucocephala	0.16±0.0	0.40±0.0	0.05±0.0	0.08±0.0
G. inodorum	0.08±0.0	0.38±0.0	0.05±0.0	0.16±0.0^{b}
C. grandis	0.07±0.0	0.18±0.0	0.07±0.0	0.05±0.0
G. pentaphyllum	0.16±0.0	0.13±0.0	0.05±0.0	0.03±0.0
C. sativum	0.05±0.0	0.09±0.0	0.02±0.0	0.02±0.0
A. graveolens	0.03±0.0	0.14±0.0	0.03±0.0	0.04±0.0
E. foetidum	0.05±0.0	0.07±0.0	0.02±0.0	0.009±0.0
C. asiatica Urban	0.04±0.0	0.16±0.0	0.02±0.0	0.03±0.0
C. ternatea	0.12±0.0	0.26±0.0	0.05±0.0	0.08±0.0
3. Herbs (2 species)				
C. quadrangularis	0.03±0.0	0.04±0.0	0.02±0.0	0.006±0.0
A. paniculata Wallex Nees	0.03±0.0	0.05±0.0	0.12±0.0^{c}	0.01±0.0
4. Fruits (6 species)				
M. sapientum	0.03±0.0	0.11±0.0	0.009±0.0	0.009±0.0
T. indica	0.29±0.0^{d}	0.15±0.0	0.13±0.0^{b}	0.07±0.0
P. guajava	0.14±0.0	0.69±0.1^{d}	0.09±0.0^{d}	0.07±0.0
M. indica	0.74±0.0^{c}	1.51±0.0^{c}	0.14±0.0^{a,b}	0.15±0.0^{c}
D. longan	1.20±0.1^{a}	1.68±0.2^{b}	0.14±0.0^{a}	0.16±0.0^{b}
P. granatum	1.11±0.1^{b}	3.13±0.1^{a}	0.03±0.0	0.24±0.0^{a}

- Values are expressed as means ± SD.
- $^{a-d}$ means in the column followed by different letters are significantly different *(P<0.05)* , ND = not determined

(0.14 mg/g) and *M. indica* (0.14 mg/g). It could be observed that the young leaf extracts of *P. granatum* exhibited the highest amounts of total phenolics and flavonoids.

3.1.2 Antioxidant activity

1,1-diphenyl-2-picrylhydrazyl (DPPH) is a stable free radical which is frequently used in measuring antioxidant activities due to its direct measurement of inhibition and its tendency for simplicity and quick analysis (Mammadov *et al*., 2011). Both solvent extracts were assessed for antioxidant activity using the DPPH radical method and the activity was expressed as percentage DPPH$^{\bullet}$ inhibition (Table 3.2). Significant differences ($p<0.05$) were found in the antioxidant activity of the plant extracts. Strong antioxidant activity was found in both the EA and ET fractions, especially those of *P. granatum* (94.1% and 95.7%), *D. longan* (94.3% and 95.5%), *M. indica* (93.9% and 94.8%), *P. guajava* (94.6% and 93.5%) and ET fraction of *M. cordifolia* Opize. (92.2%). There were strong correlations (r_{ET} = 0.779 and r_{EA} = 0.866, $p<0.05$) between antioxidant activity and phenolic content for all ethanolic (ET) and ethyl acetate (EA) extracts. This relationship indicated that the free radical scavenging activity of the plant extracts was associated with the phenolic compounds. Additionally, a high correlation (r_{ET} = 0.796) was observed between antioxidant activity and the flavonoid content in the ethanolic fractions of all plants. A moderate correlation (r_{EA} = 0.583) was observed between their ethyl acetate (EA) fractions.

3.1.3 Antiglycation activity

The antiglycation activity of the plant extracts was evaluated for the inhibition of advanced glycation end-products (AGEs) formation based on the BSA/glucose system. The results indicated that sixteen plants exhibited potential antiglycation activity (> 80% inhibition) (Table 3.2). Similarly to the antioxidant activity, strong antiglycation activity was found statistically in both the EA and ET extracts ($p<0.05$), especially those of *T. indica* (99.4% and 96.2%), *P. guajava* (99.8% and 99.8%), *M. indica* (99.8% and 99.9%), *D. longan* (99.9% and 99.8%) and *P. granatum* (99.8% and 99.0%). This correlation was also evaluated (Table 3.3). The data revealed a substantial correlation in the antiglycation activity of the plant extracts

Table 3.2 Antioxidant and antiglycation activities (BSA-glucose model) of EA and ET plant extracts of the culinary plants

Plants	DPPH radical scavenging activity (% Inhibition)		Antiglycation activity (% Inhibition)	
	EA extract	ET extract	EA extract	ET extract
1. Spices and condiments (9 species)				
M. cordifolia Opiz.	45.3±0.9^{d}	92.2±0.3^{a}	99.3±0.4^{a}	98.8±0.3^{a}
O. sanctum (green)	31.6±1.4	80.0±0.0^{b}	91.9±2.1	99.3±0.4^{a}
P. odoratum	77.8±0.7^{c}	75.9±2.3^{b}	99.7±0.1^{a}	99.8±0.0^{a}
P. sarmentosum	14.7±0.7	57.7±4.7^{c}	97.2±1.7^{b,c}	99.7±0.1^{a}
A. galangal	13.6±0.4	5.02±0.1	61.4±2.1	46.4±3.3
Z. officinale Rose.	14.1±0.7	12.0±1.6	47.5±2.1	24.3±2.7
A. cepa	1.73±0.4	3.34±0.8	58.1±6.6	71.7±0.4
A. ascalonicum	2.91±0.3	3.04±0.8	49.8±1.7	78.7±1.3
A. sativum	ND	ND	7.19±1.4	8.06±1.8
2. Vegetables (9 species)				
L. leucocephala	31.3±0.1	60.7±3.4^{b}	97.6±0.7^{b,c}	91.6±0.7^{d}
G. inodorum	87.9±0.7^{b}	53.3±1.3	97.6±0.1^{b,c}	99.5±0.2^{a}
C. grandis	ND	35.2±2.7	99.6±0.3^{a}	95.9±2.1^{c}
G. pentaphyllum	11.0±0.6	ND	98.5±0.5^{a,b}	96.3±0.2^{c}
C. sativum	6.64±0.1	28.6±0.4	82.3±2.9	85.7±2.4^{d}
A. graveolens	1.91±0.1	18.7±0.6	88.0±0.6	99.6±0.2^{a}
E. foetidum	8.82±0.4	8.87±0.5	81.0±1.1	61.8±1.6
C. asiatica Urban	9.64±0.3	59.7±4.8^{b}	82.2±4.7	95.6±1.8^{c}
C. ternatea	12.6±1.0	28.3±0.5	98.4±0.2^{a,b}	99.9±0.4^{a}
3. Herbs (2 species)				
C. quadrangularis	4.00±0.2	6.45±1.7	80.6±0.6	56.3±3.1
A. paniculata Wallex Nees	0.64±0.1	11.5±0.4	89.6±0.6^{d}	96.5±0.9^{b,c}
4. Fruits (6 species)				
M. sapientum	6.12±0.1	15.8±3.1	45.7±1.3	70.7±0.7
T. indica	23.4±1.8	17.6±1.1	99.4±0.4^{a}	96.2±0.1^{c}
P. guajava	94.6±0.2^{a}	93.5±0.9^{a}	99.8±0.1^{a}	99.8±0.0^{a}
M. indica	93.9±0.5^{a}	94.8±0.2^{a}	99.8±0.1^{a}	99.9±0.0^{a}
D. longan	94.3±0.1^{a}	95.5±0.2^{a}	99.9±0.0^{a}	99.8±0.0^{a}
P. granatum	94.1±0.3^{a}	95.7±0.2^{a}	99.8±0.0^{a}	99.0±0.0^{a}

- Values are expressed as means ± SD.
- $^{a-d}$ indicates that column followed by different letters are significantly different *(p<0.05)*
- ND = not determined

with the phenolic (r_{ET} = 0.864 and r_{EA} = 0.849) and flavonoid contents (r_{ET} = 0.796 and r_{EA}= 0.879, p<0.05). Moreover, there was high correlation in the antiglycation activities of the plant extracts with their antioxidant activities (r_{ET} = 0.707 and r_{EA}= 0.716, p<0.05). These results are noteworthy not only because the phenolic and flavonoid contents of these extracts show a positive relationship with the antioxidant activity, but also with the antiglycation property.

Table 3.3 The Pearson correlation coefficient of total phenolic and flavonoid contents with antioxidant and antiglycation activities of the culinary plant extracts

	Correlation			
	Antioxidant activity		Antiglycation activity	
	EA extract	ET extract	EA extract	ET extract
Antiglycation activity	0.716	0.707	-	-
Phenolic content	0.866	0.779	0.849	0.864
Flavonoid content	0.583	0.796	0.879	0.796

Based on the results of the screening of antioxidant and antiglycation activities in sections 3.1.2 and 3.1.3, the ethanolic extracts of some plants showed stronger inhibitory activities (> 80% inhibition). Therefore, the ethanolic extracts of 11 plant species were selected for further investigation of their antiglycation activities against glucose and methylglyoxal models providing 50% AGE inhibition (IC_{50}). In the BSA-glucose model (Figure 3.3), it was found that *P. odoratum* had significantly (p<0.05) stronger inhibitory activity than the other extracts with an IC_{50} value of 59.7 µg/mL, followed by *P. granatum*, *O. sanctum and P. sarmentosum* with IC_{50} values of 110, 130 and 135 µg/mL, respectively. However, these ethanolic extracts were less effective than aminoguanidine (IC_{50} value = 50.2 µg/mL), which was a positive control. The inhibitory effect of these selected plant extracts on the BSA-methylglyoxal (MGO) model was also determined (Figure 3.3).

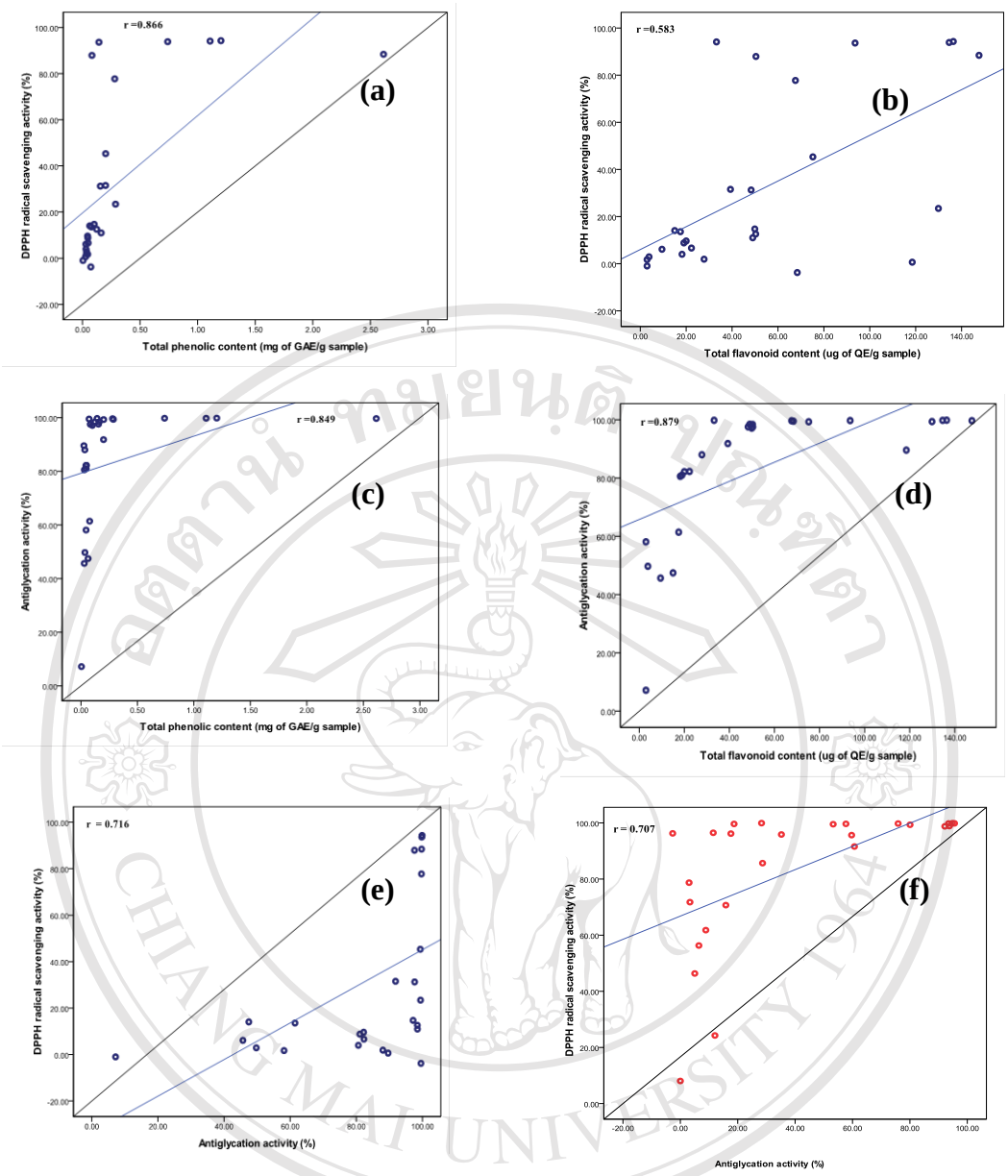

Figure 3.1 Correlation between antiglycation activity, DPPH radical scavenging activity, total phenolic and total flavonoid contents of ethyl acetate (EA) extract of culinary plants (a), DPPH radical scavenging activity *vs.* total phenolic content (b), DPPH radical scavenging activity *vs.* total flavonoid content (c), antiglycation activity *vs.* total phenolic content (d), antiglycation activity *vs.* total flavonoid content, antiglycation activity and DPPH radical scavenging of ethyl acetate (EA) extract (e) and 80% ethanol (ET) (f) of culinary plants

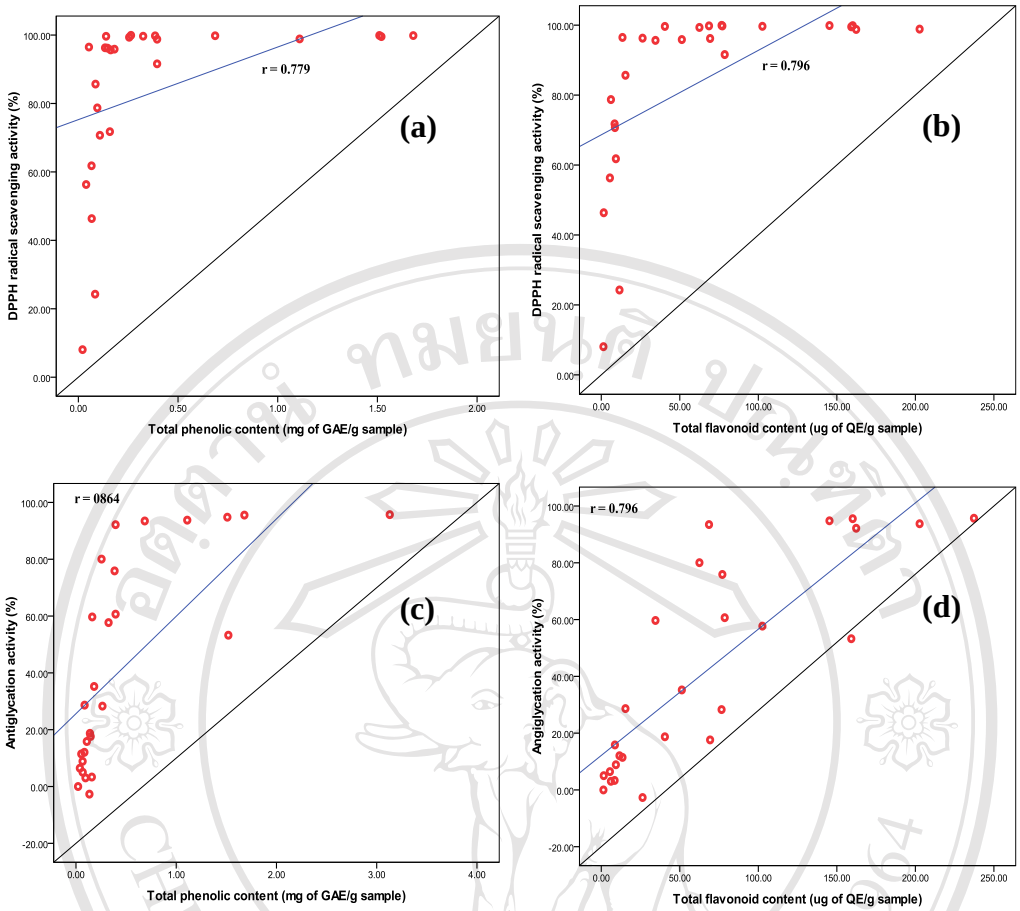

Figure 3.2 Correlation between antiglycation activity, DPPH radical scavenging activity, total phenolic and total flavonoid contents of ethanol (ET) extract of culinary plants (a), DPPH radical scavenging activity *vs.* total phenolic content (b), DPPH radical scavenging activity *vs.* total flavonoid content (c), antiglycation activity *vs.* total phenolic content (d), antiglycation activity *vs.* total flavonoid content

BSA-methylglyoxal model represented the middle stage of protein glycation in which di-carbonyl compounds such as methylglyoxal, glyoxal and 3-deoxyglucosome were more reactive in reacting with amino groups of protein leading to AGE formation. IC_{50} values showed that *M. indica* extracts (54.1 µg/mL) had statistically stronger antiglycation activity than *P. granatum*, *D. longan* and *P. guajava* (69.1, 74.2 and 93.0 µg/mL, respectively), (p<0.05). In addition, the ethanolic extracts of *M. indica*, *P. granatum* and *D. longan* had significantly (p<0.05) higher inhibitory

activity against AGE formation induced by methylglyoxal than the AG standard inhibitor (IC_{50} value = 91.2 µg/mL).

In the methylglyoxal (MGO) trapping assay, the selected plant extracts were investigated for the suppression of AGE formation through directly scavenging the reactive di-carbonyl compounds, such as MGO which are important precursors of AGEs. Each selected plant extract was incubated with methylglyoxal solution. After 0.5 and 4 h of incubation, the amount of unreacted MGO in the mixture solution was measured by HPLC analysis. As in Figure 3.4, the results showed that the strong MGO trapping ability was found in the young leaf extract of 5 plant species (*T. indica, P. guajava, M. indica, D. longan* and *P. granatum*). After 0.5 h of incubation, the ethanolic extract of *M.indica* had an obvious effect on the MGO scavenging ability with a 46.1% MGO decrease, followed by *D. longan* (34.6%), *P. guajava* (33.1%), *T. indica* (29.6%) and *P. granatum* (29.3%), respectively. The decrease of MGO was higher after 4 h of incubation. *D. longan* extract was the highest effective MGO scavenger with 87.9% MGO decrease, followed by the ethanolic extract of *P .guajava* (83.1%), *M. indica* (74.7%), *P. granatum* (72.2%) and *P. odoratum* (59.6%), respectively. The half inhibition concentration (IC_{50}) of their radical scavenging activities is illustrated in Figure 3.5. *D. longan* extract showed the highest effective radical scavenging activity with IC_{50} of 0.16 mg/mL, followed by *P. granatum* (0.16 mg/mL) and *M. indica* (0.33 mg/mL), respectively, while lower activities were found in the *T. indica* extract (IC_{50}> 5 mg/mL).

Several reference phenolic compounds (gallic acid, catechin, methyl gallate, tannic acid, chlorogenic acid, caffeic acid, rutin, *m*-coumaric acid, *o*-coumaric acid, quercetin and cinnamic acid) were used for comparative purposes in HPLC chromatogram (data not shown). HPLC chromatogram of the selected plants is shown in Figure 3.6. The results showed that their phenolic compounds could not be identified when compared with the chromatogram of the reference phenolic compounds in Table 3.4.

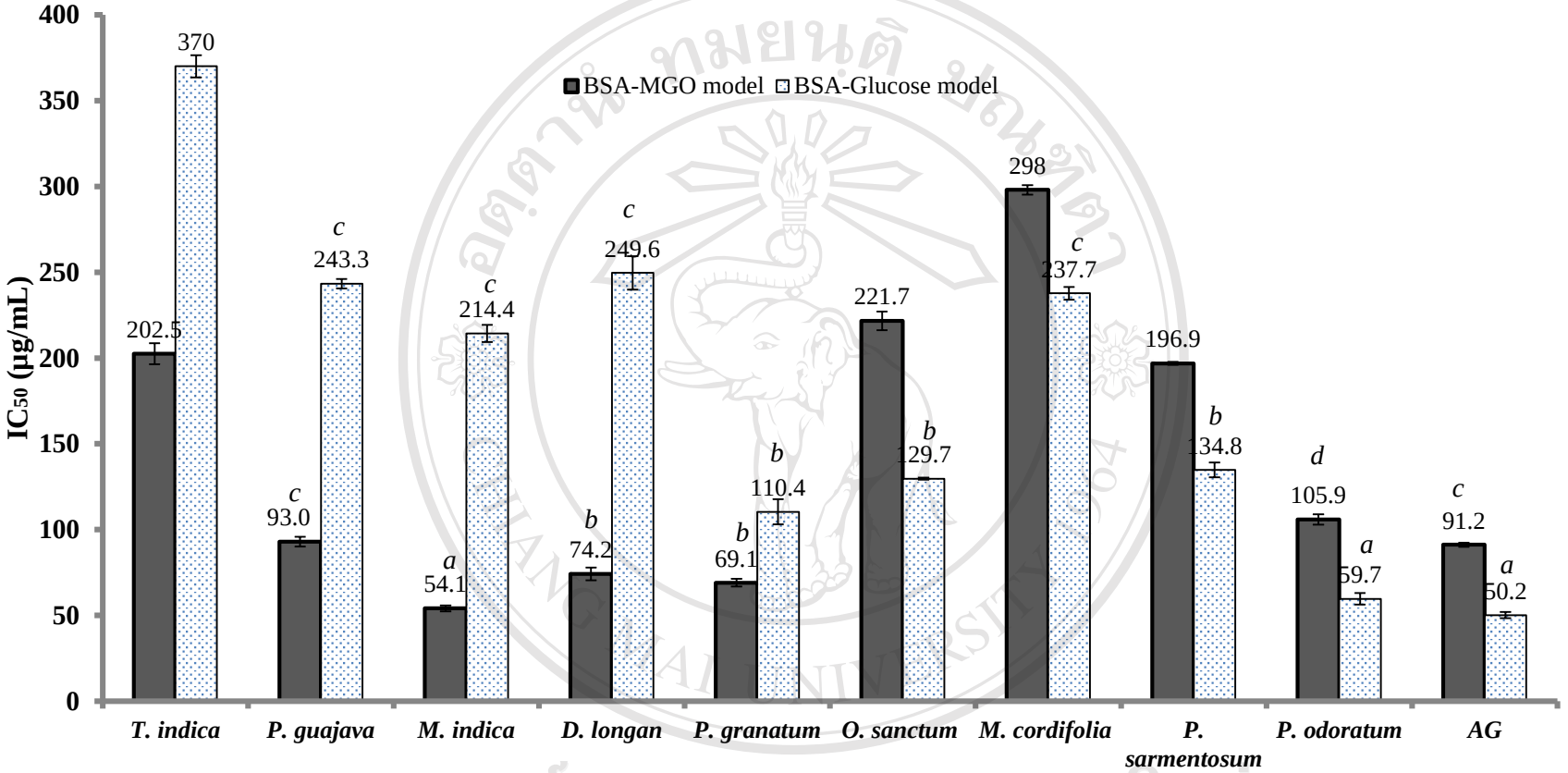

Figure 3.3 Inhibitory effect (IC_{50} value) of the selected plant extracts on the formation of glycation in BSA-glucose and BSA-methylgloxal models. Aminoguanidine (AG) was used as a positive control

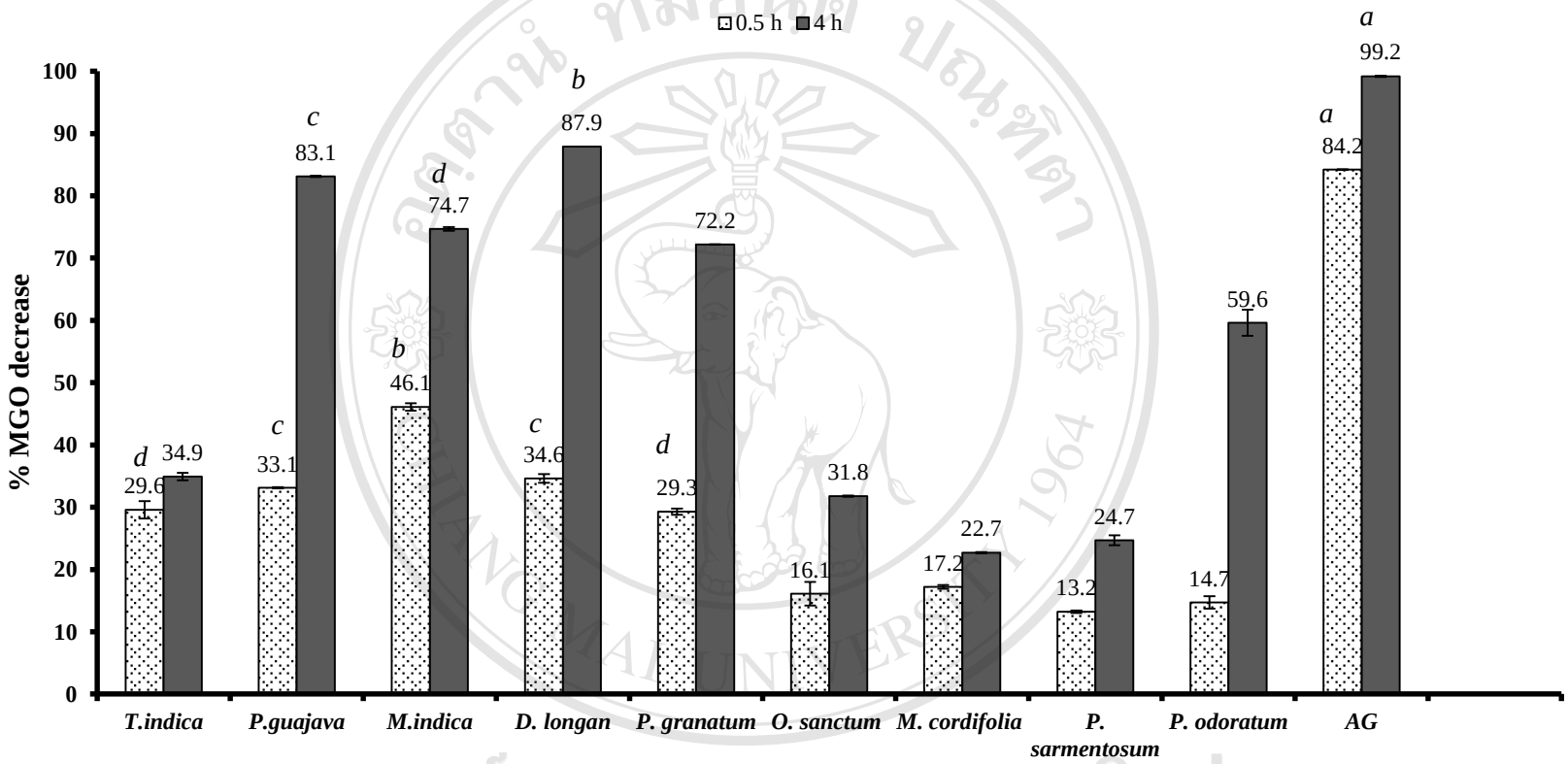

Figure 3.4 MGO trapping capacity of the selected plant extracts. The concentration of each extract is 2.0 mg/mL while the concentration of aminoguanidine (AG) is 200 µg/mL. ⬚ and ■ are incubation times of 0.5 h and 4 h, respectively

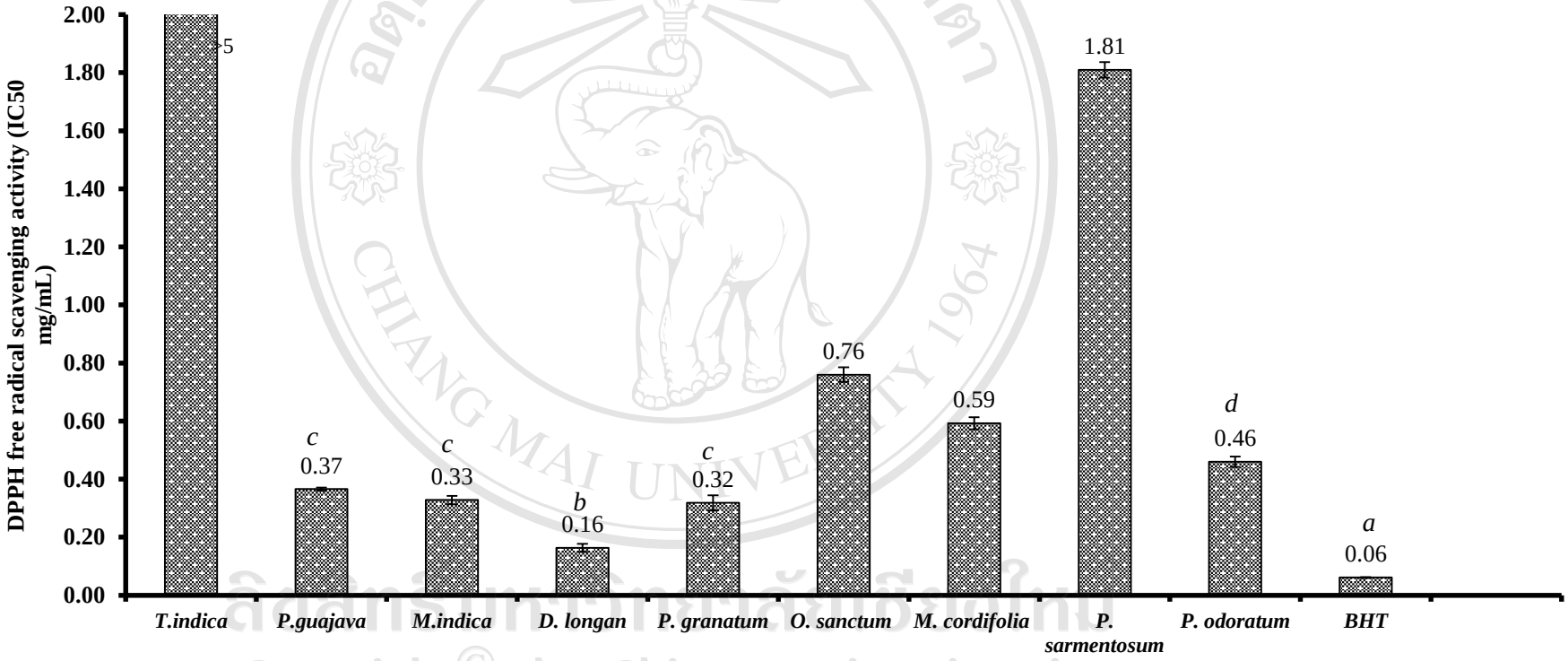

Figure 3.5 DPPH free radical scavenging activity of the selected plant extracts, BHT was used as a positive control

Table 3.4 HPLC profile of standard phenolic compounds

Standards	**Retention time (min) at 280 nm**
Gallic acid	5.126
Catechin	13.038
Methyl gallate	13.480
Tannic acid	13.650
Chlorogenic acid	14.607
Caffeic acid	16.730
Rutin	25.500
m-coumaric acid	26.744
o-coumaric acid	30.627
Quercetin	38.912
Cinnamic acid	41.483

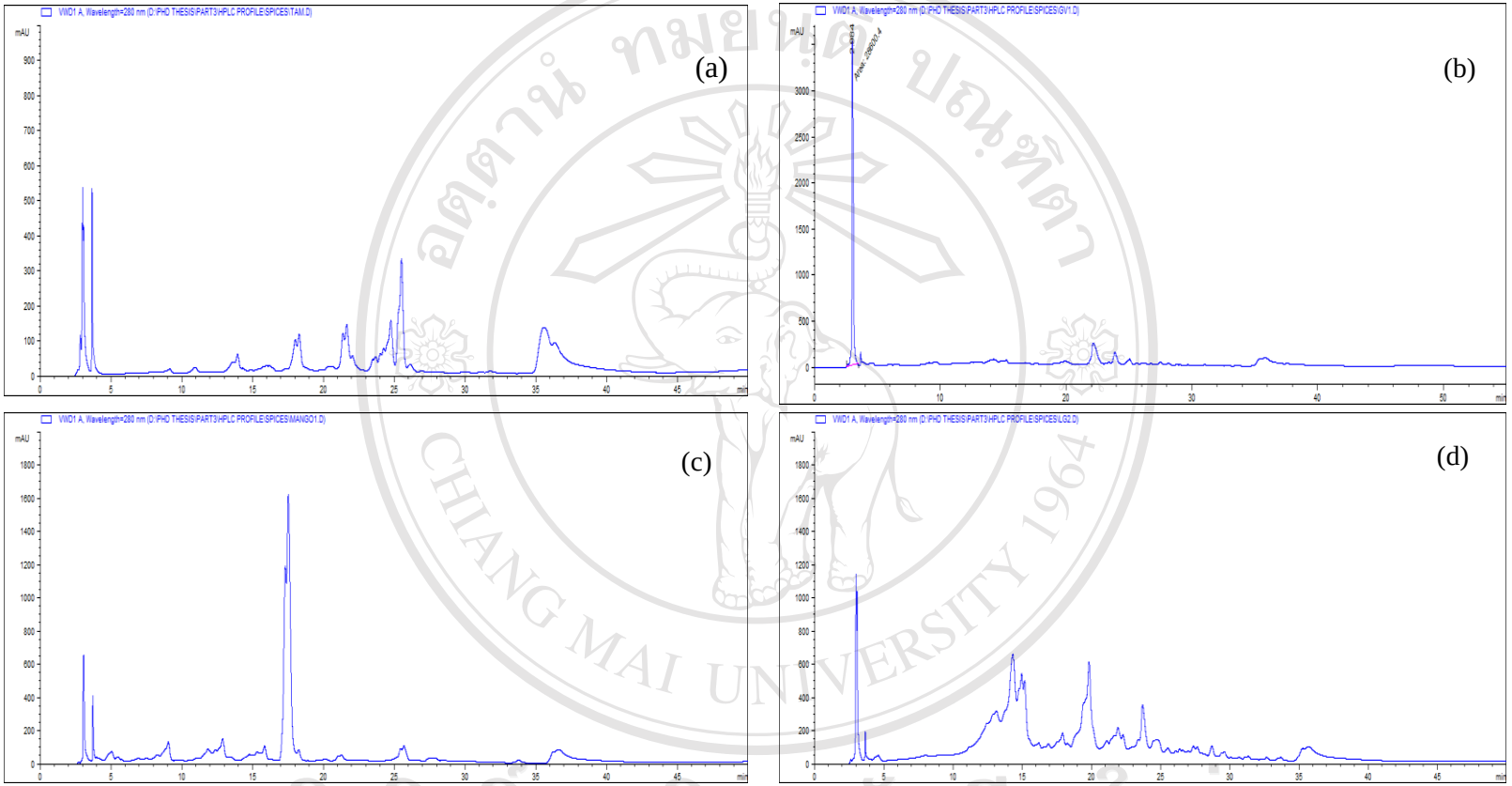

Figure 3.6 HPLC chromatograms which were unidentified of the 80% ethanolic extract from *T. indica* (a), *P. guajava* (b), *M. indica* (c) and *D. longan* (d) at 280 nm. The column was Hypersil ODS C_{18} (150x4.6mm), solvent A: 6% acetic acid in 2mM NaOAc (final pH 2.27-2.5) and Solvent B: 100% Acetronitrile. The flow rate was 0.6 mL/min

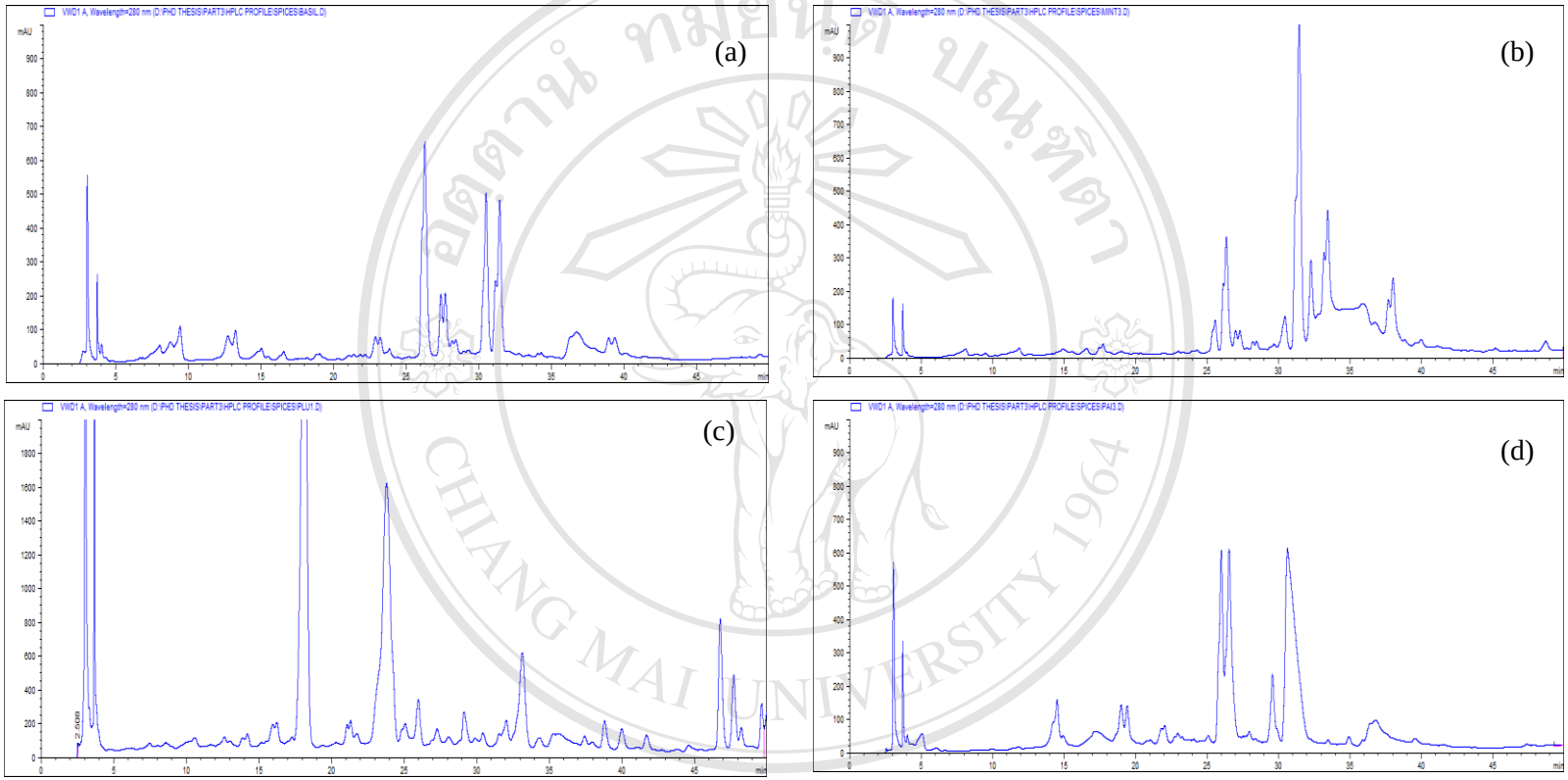

Figure 3.6 (cont.) HPLC chromatograms which were unidentified of the 80% ethanolic extract from *O. sanctum* (a), *M. cordifolia* (b), *P. sarmentosum* (c) and *P. odoratum* (d) at 280 nm. The column was Hypersil ODS C_{18} (150x4.6mm), solvent A: 6% acetic acid in 2mM NaOAc (final pH 2.27-2.5) and Solvent B: 100% Acetronitrile. The flow rate was 0.6 mL/min

3.2 Antiglycation and antidiabetic activities of Lamiaceae plant species

3.2.1 Chemical compositions of the ethanolic extract from the Lamiaceae plant species

The total phenolic contents in ethanolic extract of 5 species from Lamiaceae plants were determined by the Folin-Ciocalteu method and expressed as mg gallic acid equivalent (GAE) per gram of dried sample. Table 3.5 shows their phenolic contents ranging from 31.5 to 98.4 mg GAE/g sample. The highest content of total phenolics was observed in *O. sanctum* extract (purple) (98.4 mg/g), followed by *O. sanctum* extract (green) (71.4 mg/g) and *M.cordifolia* Opiz. (62.8 mg/g), respectively. The ethanolic extracts were also assessed for the antioxidant activity using the DPPH radical scavenging method and expressed as 50 percent of $DPPH^{\bullet}$ inhibition (IC_{50}). It was found that *M. cordifolia* Opiz. extract showed the strongest antioxidant activity with IC_{50} of 39.0 µg/mL, followed by *O. sanctum* (green) (46.9 µg/mL) and *O. sanctum* (purple) (47.0 µg/mL), respectively.

It could be observed that the Lamiaceae plant species in this experiment (Table 3.5) showed higher contained phenolic compounds than the previous result of screening (section 3.1.1) may be due to the seasonal variations for harvesting. In screening experiment, the plant samples were harvested in August, while the Lamiaceae plant species were harvested in January. This result was supported by Sivaci and Duman (2014). They found that the antioxidant activity and total phenolic compounds exhibited variations according to seasonal variations.

Table 3.5 Total phenolic content and antioxidant activity of the ethanolic extract from the Lamiaceae plant species

extract	Total phenolic content	Antioxidant activity
	mg GAE/g extract	IC_{50} (ug/mL)
O. *basilicum*	59.0 ± 4.4[c]	55.6 ± 0.1[b]
O. sanctum (purple)	98.4 ± 0.7[a]	47.0 ± 0.7[b]
O. americanum	31.5 ± 2.5	100.8 ± 0.1[c]
O. sanctum (green)	71.4 ± 1.4[b]	46.9 ± 1.9[b]
M. cordifolia Opiz.	62.8 ± 2.6[c]	39.0 ± 3.3[a]
BHT	-	6.60 ± 0.0

Values are expressed as means ± S.D.

BHT: butylated hydroxytoluene.

[a-c] means in the column followed by different letters are significantly different ($p<0.05$).

3.2.2 Characterization of phenolic compounds of the Lamiaceae plants species

Previously, rosmarinic acid, luteolin and luteolin glycosides have been reported as being generally found in the Lamiaceae family (Fecka and Turex, 2007; Gupta *et al*., 2007). Therefore, rosmarinic acid (RA), luteolin (LU) and apigenin (AP) in five ethanolic extracts of the Lamiaceae plant species were characterized using HPLC analysis. The HPLC chromatogram of the ethanolic extracts of the Lamiaceae plants was showed in Figure 3.7. The individual phenolic compounds appeared at retention times of 22.44 min for rosmarinic acid, 26.57 min for luteolin and 29.73 min for apigenin. From the HPLC chromatogram, the results showed that rosmarinic acid was found in all samples ranging from 1.31 to 8.45 mg/g (Figure 3.8). *M. cordifolia* opiz. extract contained high amounts of rosmarinic acid (8.45 mg/g), followed by *O. sanctum* (purple) extract (4.43 mg/g) and *O. sanctum* (green) extract (2.41 mg/g), respectively. Luteolin was found in *O. sanctum* (purple) and *O. sanctum* (green) extracts as 0.97 and 1.41 mg/g, respectively, whereas apigenin was also found in both *O. sanctum* (purple) (0.40 mg/g) and *O. sanctum* (green) extracts (0.96 mg/g).

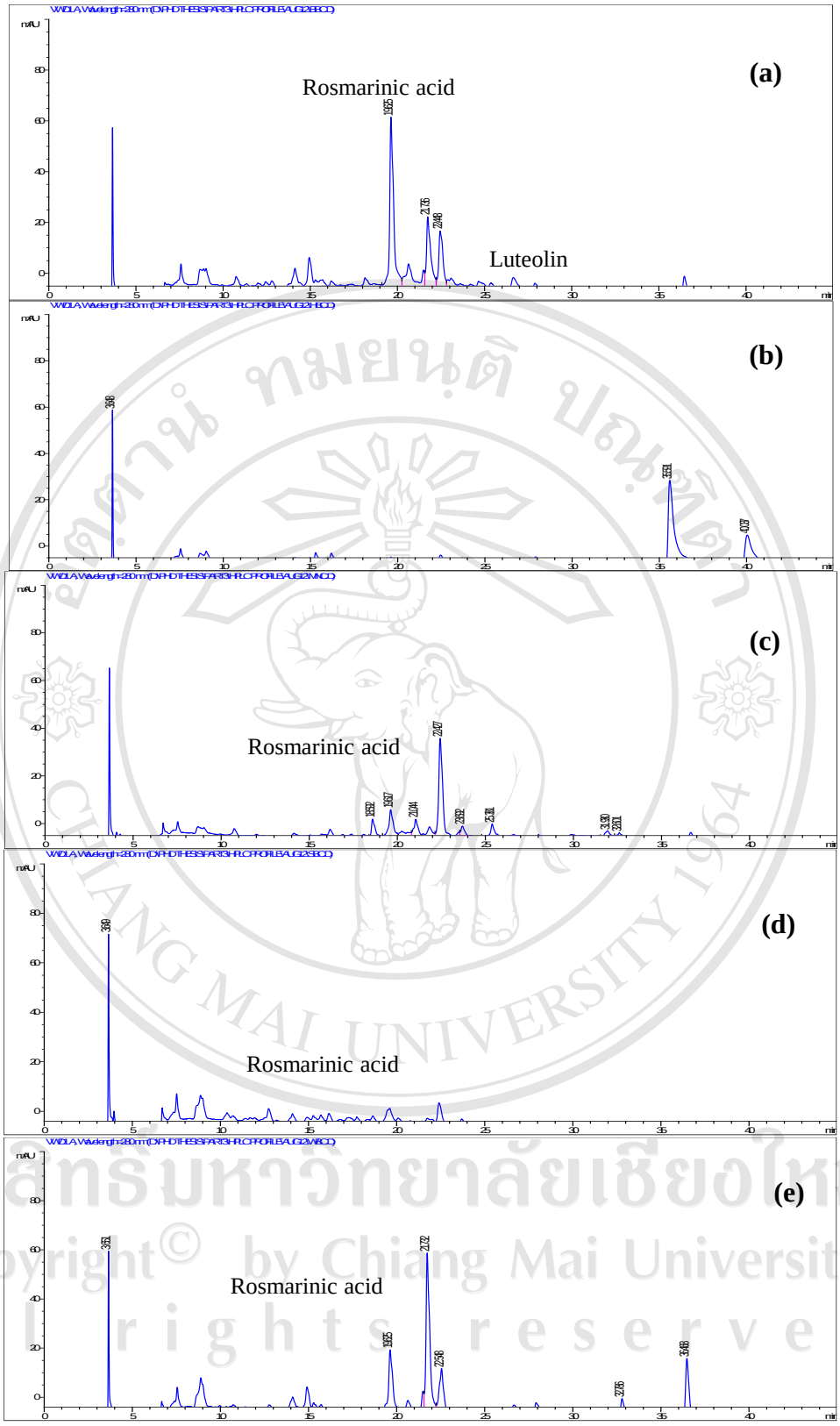

Figure 3.7 HPLC chromatogram of the ethanolic extract of *Ocimum sanctum* (purple) (a) and *Ocimum americanum* extract (b), *Metha cordifolia* Opiz. (c), *Ocimum basilicum* (d) and *Ocimum sanctum* (green) (e)

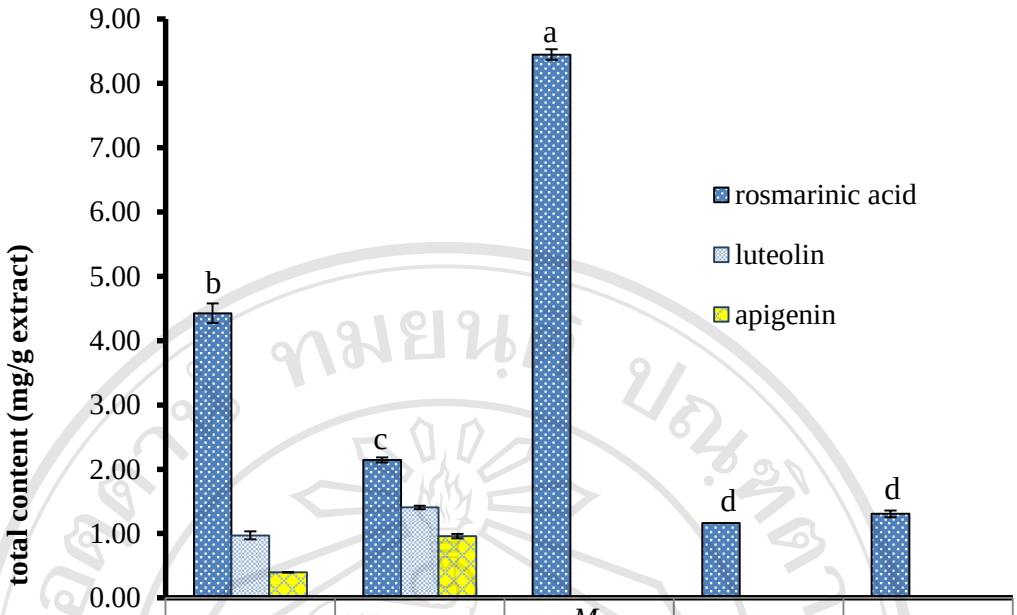

	O. sanctum (purple)	*O. sanctum (green)*	*M. cordifolia opiz.*	*O.basilicum*	*O. americanum*
rosmarinic acid	*4.43*	*2.14*	*8.45*	*1.16*	*1.31*
luteolin	*0.97*	*1.41*	*0.00*	*0.00*	*0.00*
apigenin	*0.40*	*0.96*	*0.00*	*0.00*	*0.00*

Figure 3.8 Amounts of rosmarinic acid, luteolin and apigenin in ethanolic extracts of the Lamiaceae plants

3.2.3 Determination of α-glucosidase (maltase) inhibition of the Lamiaceae plant species

The inhibition of α-glucosidase plays an important role in control of the blood glucose levels of diabetes and its complications. The rat intestinal α-glucosidase inhibitory activity was determined by measuring concentration of glucose released from the maltose substrate. Table 3.6 shows the α-glucosidase (maltase) inhibition of the ethanolic extract from the Lamiaceae plant species. It was found that the *O. sanctum* (purple) showed the strongest inhibition with IC_{50} of 1.42 mg/mL, followed by *O. basilicum* (IC_{50} = 1.46 mg/mL) and *M. codifolia* Opiz. (IC_{50} = 1.56 mg/mL), respectively.

Table 3.6 α-glucosidase (maltase) inhibition and antiglycation activities of the ethanolic extracts from Lamiaceae plants

Ethanolic extract	α-glucosidase (maltase) inhibition IC_{50}(mg/mL)	Antiglycation activity IC_{50} (mg/mL)	
		BSA-MGO model	Histone-MGO model
O. basilicum	1.46 ± 0.1^{a}	0.850 ± 0.0^{b}	1.02 ± 0.1^{b}
O. americanum	5.06 ± 0.0^{d}	0.700 ± 0.0^{c}	>2.0
O. sanctum (green)	2.62 ± 0.0^{c}	0.769 ± 0.1^{b}	1.11 ± 0.1^{c}
M. cordifolia Opiz.	1.56 ± 0.0^{b}	1.10 ± 0.6^{d}	0.918 ± 0.1^{b}
O. sanctum (purple)	1.42 ± 0.0^{a}	0.402 ± 0.0^{a}	0.645 ± 0.0^{a}
aminoguanidine	-	0.092 ±0.0	0.074 ± 0.0

Values are expressed as means ± S.D.

$^{a-c}$ means in the column followed by different letters are significantly different ($p<0.05$).

3.2.4 Determination of antiglycation activities of the Lamiaceae plant species

3.2.4.1 Antiglycation activities of the Lamiaceae plant species in extracellular (BSA-MGO) and intracellular (histone-MGO) proteins

The abilities of five ethanolic extracts from the Lamiaceae plant species to inhibit AGEs formation were evaluated using the BSA-MGO and histone-MGO models. As is well-known, MGO, an intermediate of AGE formation, can induce crosslinking of both extracellular and intracellular proteins in the body's tissue. BSA, which is a serum protein, was considered to be an extracellular model protein. Whereas histone, which is a composition of the chromosome structure in the nucleus, is the targeted protein glycation for intracellular model proteins due to the fact that it contains a very rich amount of arginine and lysine residues. After a week of incubation time, the formation of AGE fluorescence induced by MGO was measured at an excitation wavelength of 370 nm and an emission wavelength of 440 nm using a luminescence microplate reader. Table 3.6 shows the inhibitory effects of the ethanolic extracts from five Lamiaceae plants on the AGE formation in both BSA-MGO and histone-MGO

models. Among the ethanolic extracts, the *O. sanctum* (purple) extract demonstrated the strongest inhibitory effect against AGE formation in both BSA-MGO and histone-MGO models when compared with the other extracts, with IC_{50} values of 0.402 mg/mL and 0.645 mg/mL, respectively. However, the IC_{50} values of these extracts were less effective than aminoguanidine (AG), which is an antiglycative standard inhibitor in both model proteins (IC_{50} values of 0.092 and 0.074 mg/mL). It has been observed that the ethanolic extract of *O. sanctum* (purple) not only showed the strongest α-glucosidase (maltase) inhibition, but also showed the most effective ability against AGE formation in both extracellular and intracellular model proteins.

3.2.4.2 Analysis of protein conformation changes by sodium dodecyl sulfate poly acrylamide gel electrophoresis (SDS-PAGE)

Gel electrophoresis was used to confirm the AGE inhibitory effect of the ethanolic extracts of Lamiaceae plants on the crosslinking of histone reacted with MGO. Figure 3.9 shows the SDS-PAGE profiles for histone (intracellular model protein) incubated with the absence (control) or presence of different concentrations of methylgyloxal (MGO). The SDS-PAGE profile of histone glycation correlated with their fluorescent intensity (Figure3.10(a)) measured by luminescent microplate reader. The results show that the native band of histone mainly performed at 14 KDa as a monomer form at lane 1 (Figure3.10(b)). While, the dimeric form of histone clearly appeared to increase at 30 KDa after incubation with methylgloxal (5mM) at 37°C for a week (lane 3). The addition of luteolin (LU), an authentic phenolic compound, at a concentration of 40 µg/mL markedly inhibited the cross-linking of histone (lane 2). The addition of *O. sanctum* (purple; BB), *M. cordifolia* Opiz. (MN), *O. americanum* (HB), *O. basilicum* (SB) and *O. sanctum* (green; WB) extracts at 600 µg/mL (lane 4-8) showed a decrease in the cross-linking of the histone. The results suggested that all Lamiaceae plant extracts effectively inhibitied the AGE formation and this was confirmed by visualization on gel eletrophoresis.

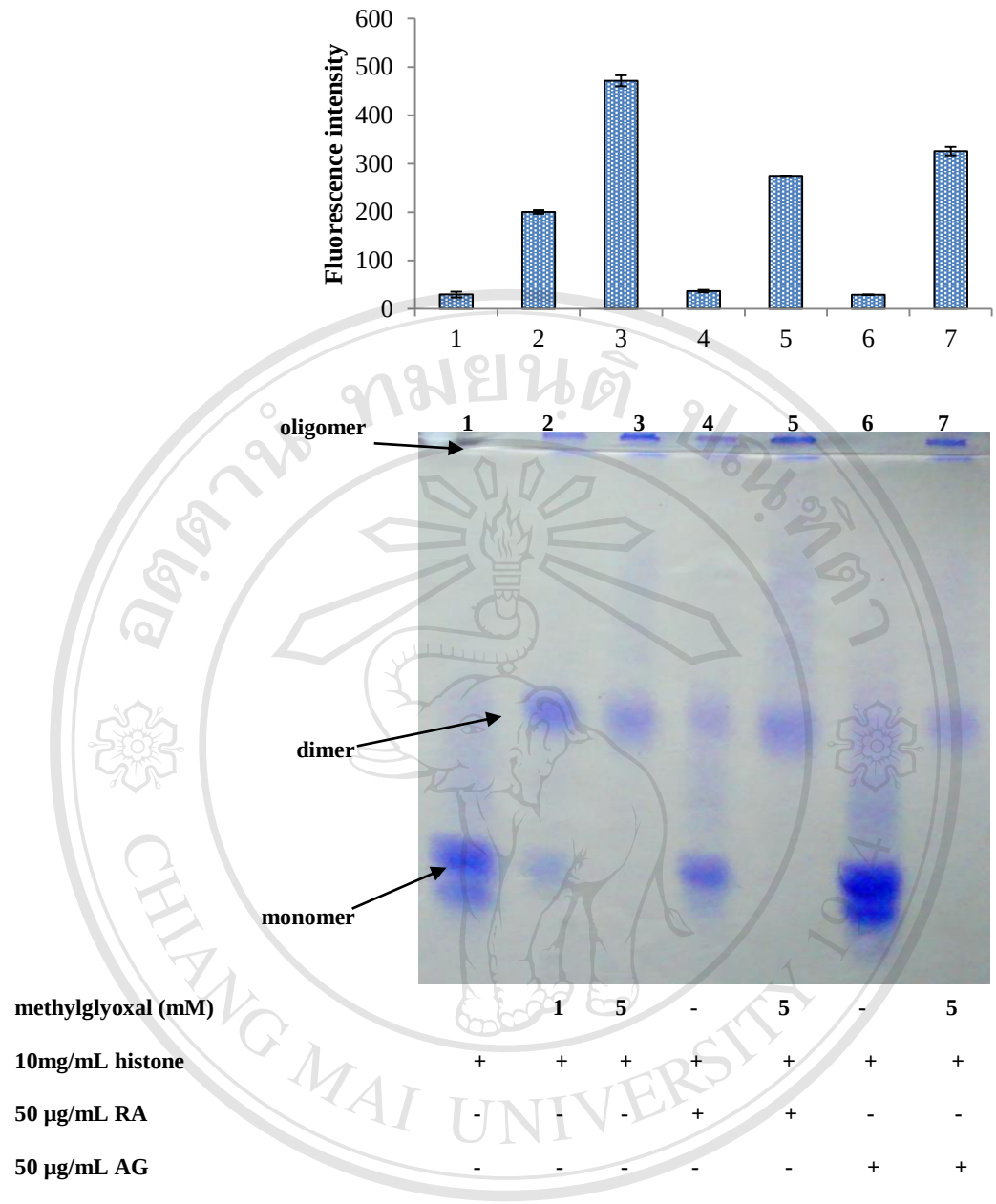

Figure 3.9 SDS-PAGE Commassie stained gel profile of glycated histone. The native band of histone represented by lane 1. Lanes 2 and 3 represent the cross-linked band of histone (10 mg/mL) when it was incubated with 1 and 5 mM of methylglyoxal, respectively. The band of histone was incubated with or without 5 mM methylglyoxal in the presence of inhibitors; 50 µg/mL of rosmarinic acid (RA) (lane 4 and 5) and 50 µg/mL of aminoguanidine (AG) (lane 6 and 7).

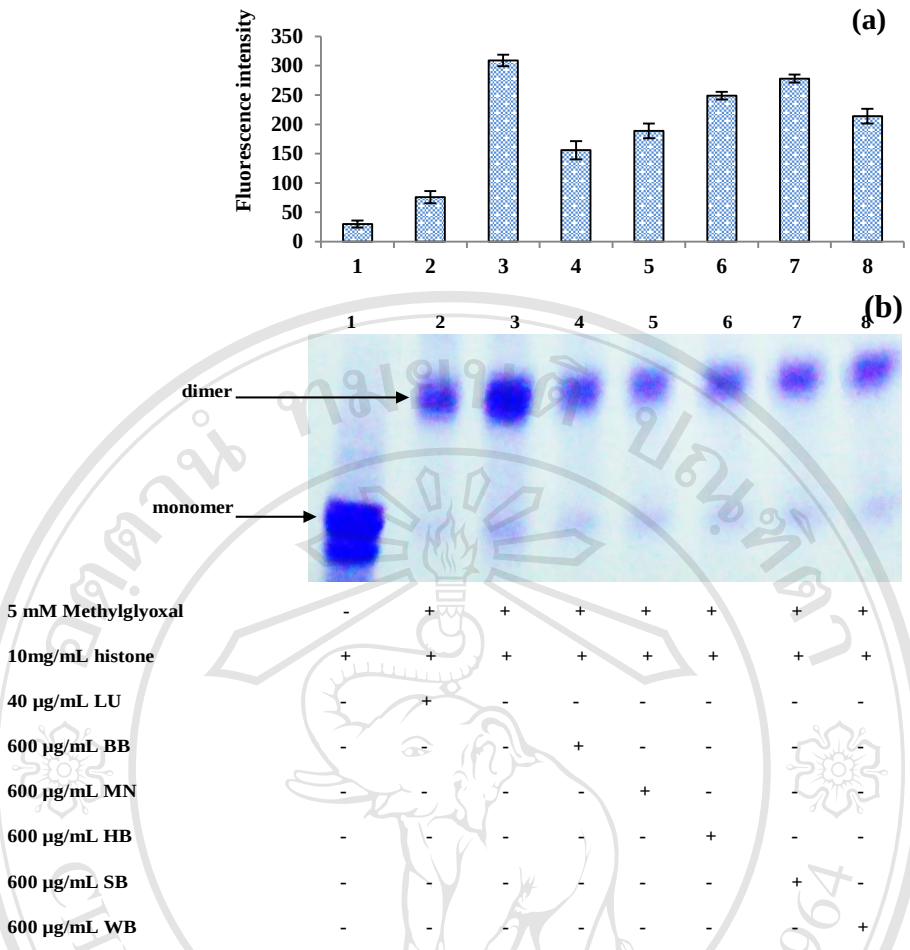

Figure3.10 AGE inhibition -mediated protein crosslinks of the Lamiaceae plants. (a) AGE fluorescence intensity of glycated histone and (b) representative SDS-PAGE Coomassie stained gel profile of histone incubated with/without 5 mM of methylglyoxal in the presence and absence of the Lamiaceae plant extracts; lane 1, histone alone; lane 2, histone+MGO+40 µg/mL of luteolin; lane 3, histone+MGO; lane 4-8, histone+MGO+600 µg/mL of the ethanolic extract of *Ocimum sanctum* (purple), BB; *Metha cordifolia* Opiz., MN; *Ocimum americanum*, HB; *Ocimum basilicum*, SB and *Ocimum sanctum* (green),WB, respectively.

3.3 Partial purification and identification of phenolic compounds from *Ocimum sanctum* (purple) extract

Based on the results of the screening of antiglycation activity and α-glucosidase (maltase) inhibition in sections (3.2.3 and 3.2.4), the most active species under the Lamiaceae family against AGE formation was found in the ethanolic extract from *O. sanctum* (purple). Therefore, this extract was of interest for the further study of its antiglycative compounds, particularly the phenolic compounds.

The ethanolic crude extract from *O. sanctum* (purple) was subsequently partitioned in ethyl acetate (EA) and water (aqueous) fractions. The total phenolic content of these fractions was determined by Folin-Ciocalteu method using gallic acid as the standard equivalent. Moreover, these fractions were also assessed for the antioxidant and antiglycation activities and α-glucosidase inhibition.

These results showed that the highest amount of phenolic content was found in the EA fraction of *O. sanctum* (purple) (17.06 mg/g of crude sample), while its aqueous fraction showed a low amount of phenolic content (0.88 mg/g of crude sample) **(**Table 3.7). In addition the EA fraction of *O. sanctum* (purple) also exhibited the highest effective antioxidant activity with IC_{50} value of 61.7 µg/mL, followed by its aqueous fraction (119.6 µg/mL), respectively. Similarly to the antioxidant activity, the EA fraction of *O. sanctum* (purple) showed the stronger antiglycation activity in both BSA-MGO and histone-MGO models with IC_{50} values of 0.294 and 0.290 mg/mL, respectively, whereas no activity was found in its aqueous fraction in the BSA-MGO model and low inhibitory activity was observed in the histone-MGO model (0.804 mg/mL).

The anti-diabetic activity of these fractions was evaluated through the inhibition of α-glucosidase (maltase) leading to a decrease in the absorption of glucose to cells. The EA fraction showed significantly stronger inhibitory activity (IC_{50}= 0.569 mg/mL) than the aqueous fraction. Therefore, the EA fraction of this plant was selected for further investigation.

Table 3.7 Total phenolic content, antioxidant and antiglycation activities and α-glucosidase inhibition of *Ocimum sanctum* (purple).

O. sanctum (purple) Extract	Total phenolic content (mg GAE/g extract)	DPPH radical scavenging activity IC_{50} (mg/mL)	α-glucosidase (maltase) inhibition IC_{50} (mg/mL)	Antiglycation IC_{50} (mg/mL)	
				BSA-MGO model	Histone-MGO model
Crude extract	98.4±0.7	47.0±0.7	1.42±0.0	0.402±0.0	0.645±0.0
- EA fraction	17.06±0.0	61.7±0.1	0.569±0.0	0.294 ± 0.0	0.290±0.0
- Aqueous fraction	0.88±0.0	119.6±0.1	ND	ND	0.804±0.0

- EA is ethyl acetate
- ND is not detected

3.3.1 Separation and partial purification of *Ocimum sanctum* (purple) by silica gel 60 column chromatography

The ethyl acetate extract (10.0 g) was separated by flash CC over silica gel (Merck 7734, Mesh 70-230, 250 g; column diameter 7 cm. x height 15 cm.). Gradient elution (Table 3.8) was conducted initially with 100% n-hexane, gradually increased ethyl acetate (5% every 400 mL), followed by an increase of methanol in ethyl acetate and finally with 100% methanol to afford 17 fractions, F_1-F_{17}. All fractions obtained from the column were monitored by TLC and the bands were observed under UV light.

Table 3.8 Fractionation yields from ethyl acetate extract of *Ocimum sanctum* (purple)

fraction	Weight (g)	%yield	phase	No.	Elution system	Volume of elution (mL)
F_1	0.249	2.4	Oil	4-8	Hex:EA=85:15	400
F_2	0.254	2.5	Oil	9-10	Hex:EA=80:20	400
F_3	0.164	1.6	Oil	11-13	Hex:EA=75:25	400
F_4	0.285	2.8	Oil	14-17	Hex:EA=75:25	400
F_5	0.907	9.0	solid	18-22	Hex:EA=70:30	400
F_6	0.468	4.6	solid	23-26	Hex:EA=65:35	400
F_7	0.795	7.9	solid	27-31	Hex:EA=60:40	400
F_8	0.481	4.8	solid	38-42	Hex:EA=50:50	400
F_9	0.400	4.0	solid	43-47	Hex:EA=40:60	400
F_{10}	0.689	6.8	solid	48-65	Hex:EA=35:65	400
F_{11}	0.855	0.8	solid	66-67	Hex:EA=20:80	400
F_{12}	1.112	11.1	solid	68-81	Hex:EA=15:85	400
F_{13}	0.493	4.9	solid	82-87	Hex:EA=5:95	400
F_{14}	0.243	2.4	solid	88-96	100% EA	400
F_{15}	0.228	2.2	solid	97-102	EA:ME=20:80	400
F_{16}	0.376	3.7	solid	103-107	EA:ME=10:90	400
F_{17}	1.836	18.4	solid	108-115	100% methanol	1,200
Total	9.835	89.9	-	-	-	-

Hex: hexane, EA: ethyl acetate, ME: methanol

3.3.2 Determination of antiglycation activity and α-glucosidase (maltase) inhibition of the separated fractions of *Ocimum sanctum* (purple)

The antiglycation activity of all fractions of *O. sanctum* (purple) separated on the silica gel 60 column are shown in Figure 3.11. Their inhibitory effects at a concentration of 250 µg/mL were assessed on the AGE formation after a week of incubation in the BSA-MGO model system by measuring the fluorescence of their reaction mixture at an excitation wavelength of 370 nm and an emission wavelength of 440 nm. Among these fractions, the results showed that the separated fractions F11, F16 and F10 had stronger antiglycation effects (50.0, 45.7 and 44.2%, respectively)

than the crude extract (42.5%) at a concentration of 250 µg/mL, whereas the oil fractions F1-F4 displayed antiglycation activity when compared with the other fractions. However, these fractions had less effective inhibitory than the standard phenolic compounds; rosmarinic acid (42.5%) and luteolin (70.5%) at a concentration of 25 µg/mL.

The intestinal α-glucosidase (maltase) inhibition of these fractions was also determined. Figure 3.12 demonstrated the IC_{50} values of the EA crude extract and all separated fractions of *O. sanctum* (purple) against intestinal α-glucosidase using maltose as a substrate. The results showed that the fraction F16 displayed the most effective intestinal maltase inhibition (IC_{50} = 0.443 mg/mL), whereas some fractions (F15, F14, F17, F10 and F12) showed moderate α-glucosidase (maltase) inhibition. Other fractions exhibited lower potential inhibitory activities. However, all fractions were less potential than rosmarinic acid (IC_{50} = 0.032 mg/mL).

3.3.3 Thin layer chromatography (TLC) and high performance liquid chromatography (HPLC) analyses of the separated fractions of *Ocimum sanctum* (purple)

In order to investigate the separated fractions, each fraction was analyzed by TLC and HPLC. Based on our previous experiment, the preliminary identification of *O. sanctum* (purple) revealed the identified phenolic compounds (luteolin, apigenin and rosmarinic acid). Therefore, these identified phenolic compounds were used for comparative purposes in the TLC and HPLC analyses. Generally, phenolic compounds appeared dark under UV light (254 and 365 nm). It was found that the separated fractions F1, F2, F5, F6, F7, F9-F17 from *O. sanctum* (purple) showed dark spots under UV light (Table 3.9). Preliminary identification of these separated fractions was based on comparison of its retention time with those of the authentic phenolic compounds that showed the fractions F9-F11, mixed compounds and exhibited R_f values at 0.800 and 0.675 which were similar to the R_f values of apigenin (0.800) and luteolin (0.675). Whereas fraction F16 and F17 showed R_f value at 0.810 which was similar to rosmarinic acid. Moreover, all fractions were analyzed by HPLC technique as is shown in Figure 3.13. The results showed that fraction F9 exhibited a major peak

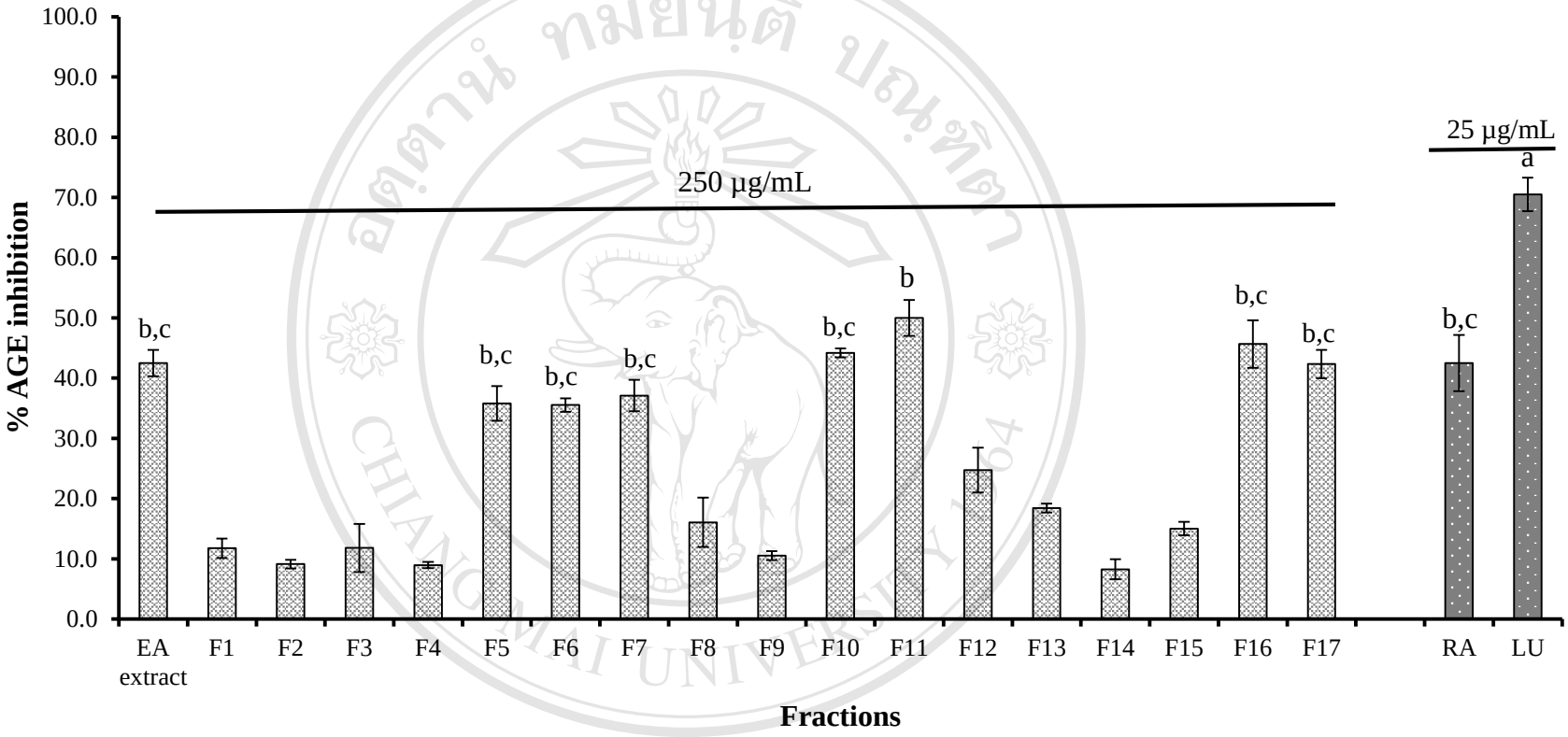

Figure 3.11 % AGE inhibition in BSA-MGO model of the fractions (F1-F17) of crude EA fraction of *Ocimum sanctum* (purple) at concentration of 250 µg/mL separated by silica gel column chromatography. Rosmarinic acid (RA) and luteolin (LU) were used as AGE standard inhibitors at the concentration of 25µg/mL

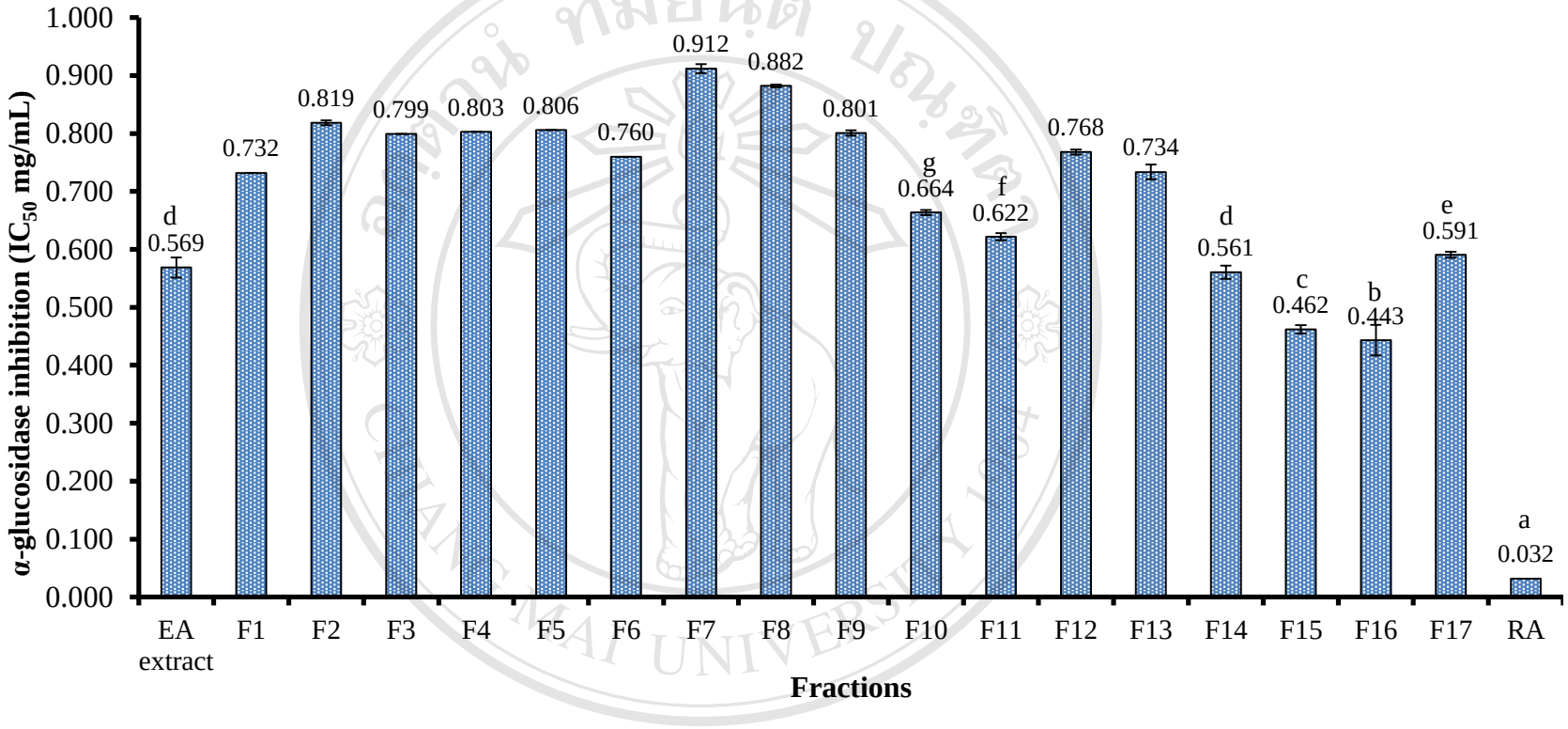

Figure 3.12 IC_{50} value (mg/mL) of α-glucosidase (maltase) inhibition of the fractions (F1-F17) of crude EA fraction of *Ocimum sanctum* (purple) separated by silica gel 60 column chromatography. Rosmarinic acid (RA) was used as a standard inhibitor

at 26.201 min on the chromatogram. Preliminary identification of F9 was based on a comparison of the retention time with the authentic compounds, and it was identified as apigenin. Whereas, both fractions F10 and F11 that revealed a major peak at 23.301 min were identified as luteolin. The fraction F16 and F17 showed a single peak at 19.594 min which was primarily identified as rosmarinic acid.

Table 3.9 R_f values and color appearances on TLC chromatograms of the fractionated fractions from the ethyl acetate extract of *Ocimum sanctum* (purple)

Fraction	R_f value in solvent system*			Color under UV light		Color appearance
	a	b	c	254	365	
F1, 4 spots						
− F1A	0.243	-	-	Brown(+)	-	Brown (+)
− F1B	0.463	-	-	Brown(+)	-	Yellow (+)
− F1C	0.756	-	-	Dark purple(+++)	Yellow(+)	Yellow(+)
− F1D	0.878	-	-	Brown(+++)	Yellow(+)	Yellow (+++)
F2, 1 spot	0.463			Dark purple(+++)	Orange(+)	Yellow(+)
F3, 2 spots						
- F3A	0.390	-	-	Brown(++)	Orange(+)	Dark green (+)
- F3B	0.463	-	-	Brown(++)	Orange(+)	Yellow (+)
F4, 4 spots						
- F4A	0.268	-	-	Brown(+)	Orange(+)	Dark green (+)
- F4B	0.341	-	-	Brown(+)	Yellow(+)	Yellow (+)
- F4C	0.390	-	-	Brown(+)	-	Yellow (+)
- F4D	0.463	-	-	Brown(+)	-	Yellow (+)
F5, 2 spots						
- F5A	0.525	-	-	Brown(+)	Orange(++)	Yellow (+)
- F5B	0.775	-	-	Dark purple(+++)	Dark(++)	Dark green(+++)
F6, 3 spots						
- F6A	0.575	-	-	Dark purple(++)	Dark (++)	Yellow (+++)
- F6B	0.725	-	-	Brown(++)	Orange(+)	Dark green(+++)
- F6C	0.775	-	-	Brown(++)	Orange(+)	Dark green(+++)

TLC system: a: Hexane:ethyl acetate=7:3; b: Hexane:ethyl acetate= 1:9; c: ethyl acetate:methanol=5:5

Table 3.9 (cont.) R_f values and color appearances on TLC chromatograms of the fractionated fractions from the ethyl acetate extract of *Ocimum sanctum* (purple)

Fraction	R_f value in solvent system*			Color under UV light		Color appearance
	a	b	c	254	365	
F7, 4 spots						
- F7A	0.400	-	-	Brown(++)	Orange (+)	Yellow (++)
- F7B	0.550	-	-	Dark purple (+++)	Dark (++)	Dark green (+++)
- F7C	0.675	-	-	Brown(++)	Orange (++)	Yellow (++)
- F7D	0.725	-	-	Brown(++)	Orange (++)	Yellow (++)
F8, 4 spots						
- F8A	0.375	-	-	Brown(++)	Orange (++)	Yellow (+++)
- F8B	0.425	-	-	Brown(++)	Orange (++)	Yellow (++)
- F8C	0.500	-	-	Brown(++)	Orange (++)	Yellow (++)
- F8D	0.575	-	-	Brown(++)	Orange (++)	Dark green (++)
F9, 2 spots						
- F9A	-	0.800	-	Dark purple (+++)	-	Yellow (+)
- F9B	-	0.950	-	Brown(+)	Orange (++)	Green (+)
F10, 2 spots						
- F10A	-	0.675	-	Dark purple (+++)	-	Yellow (+)
- F10B	-	0.800	-	Dark purple (+++)	-	Yellow green (+)
F11, 3 spots						
- F11A	-	0.300	-	Brown (++)	Orange (+)	Dark green (++)
- F11B	-	0.525	-	Dark purple (+++)	-	Yellow (+)
- F11C	-	0.675	-	Dark purple (++)	-	-
F12, 2 spots						
- F12A	-	0.525	-	Dark purple (+)	Bright(+)	Dark green (++)
- F12B	-	0.600	-	Brown (++)	Orange (+)	Yellow (+)

TLC system: a: Hexane:ethyl acetate=7:3; b: Hexane:ethyl acetate= 1:9; c: ethyl acetate:methanol=5:5

Table 3.9 (cont.) R_f values and color appearances on TLC chromatograms of the fractionated fractions from the ethyl acetate extract of *Ocimum sanctum* (purple)

Fraction	R_f value in solvent system*			Color under UV light		Color appearance
	a	b	c	254	365	
F13, 1 spot						
- F13A	-	0.15	-	Brown (+++)	Orange (+++)	Dark green (++)
F14, 2 spots						
- F14A	-	-	0.825	Brown (++)	Orange (+++)	Green (+)
- F14B	-	-	0.975	Brown (+++)	Orange (+++)	Brown (++)
F15, 2 spots						
- F15A	-	-	0.825	Brown (++)	Orange (+++)	Green (+)
- F15B	-	-	0.975	Brown (++)	Orange (+++)	Brown (++)
F16, 2 spots						
- F16A	-	-	0.810	Brown (++)	Blue(++)	Brown (+)
- F16B	-	-	0.976	Brown (++)	Orange (++)	Brown (++)
F17, 2 spots						
- F17A	-	-	0.810	Brown (++)	Blue (+++)	Brown (+)
- F17B	-	-	0.976	Brown (++)	Orange (+++)	Brown (+)
Rosmarinic acid	-	-	0.810	Purple (+++)	Blue (++)	Brown (+)
Apigenin	-	0.800	-	Purple (+++)	Bright yellow(++)	Yellow (+)
Luteolin	-	0.675	-	Purple (+++)	Bright yellow (++)	Yellow (+)

TLC system: a: Hexane:ethyl acetate=7:3; b: Hexane:ethyl acetate= 1:9; c: ethyl acetate:methanol=5:5

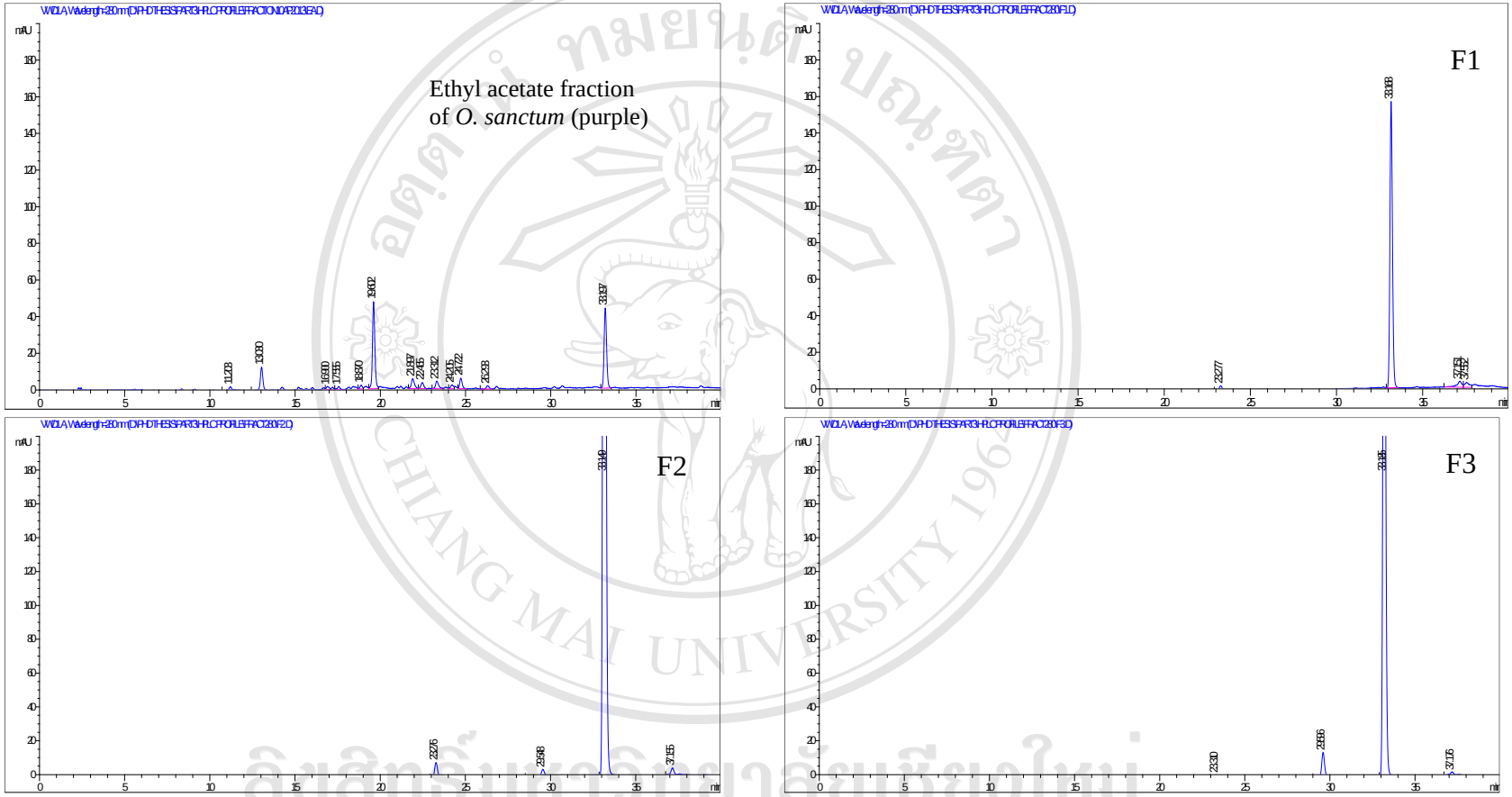

Figure 3.13 HPLC chromatograms of the crude ethyl acetate (EA) fraction of *Ocimum sanctum* (purple) and the fractions separated on the silica gel 60 column chromatography

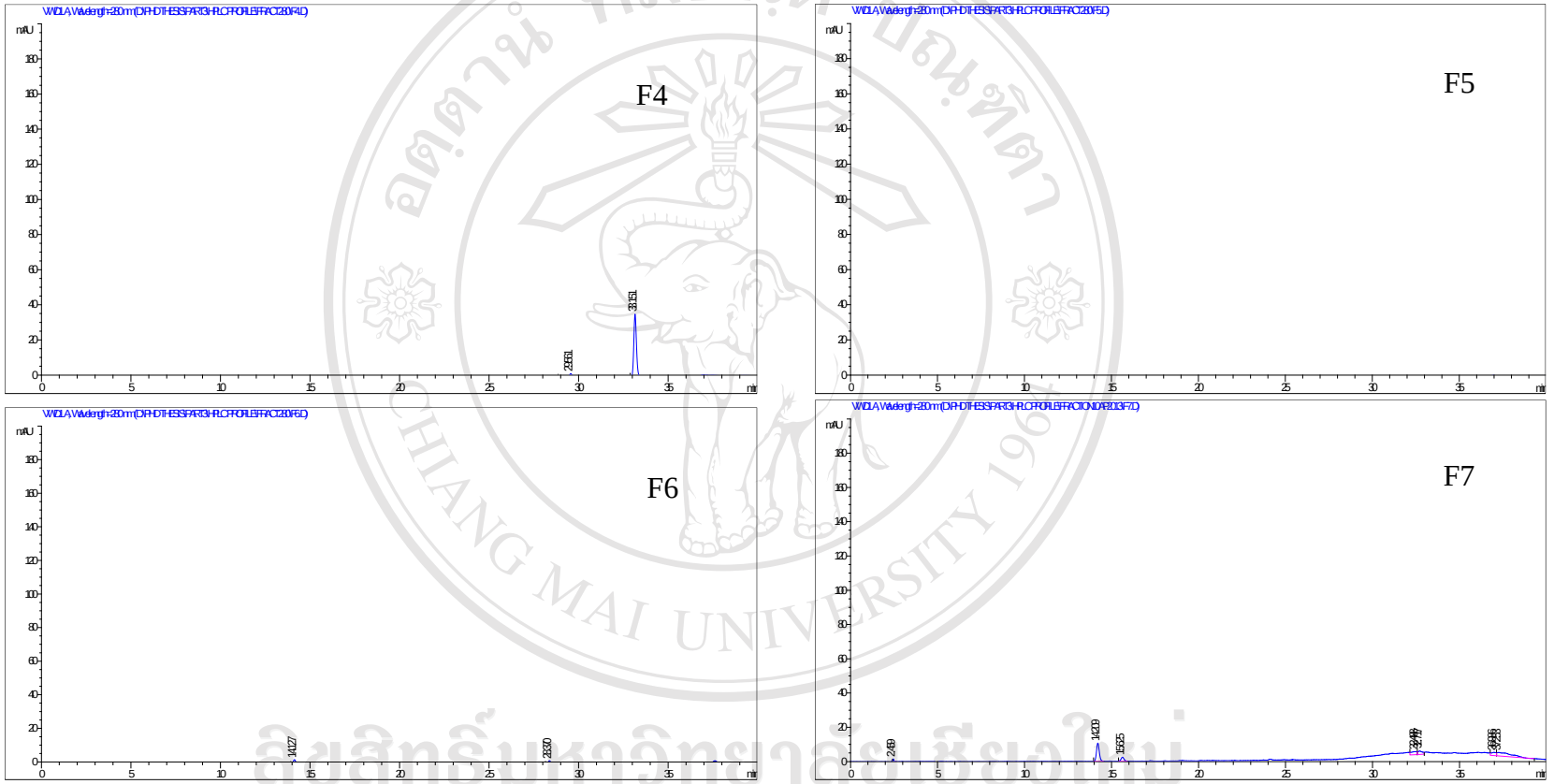

Figure 3.13 (cont.) HPLC chromatograms of the fractions separated on the silica gel 60 column chromatography

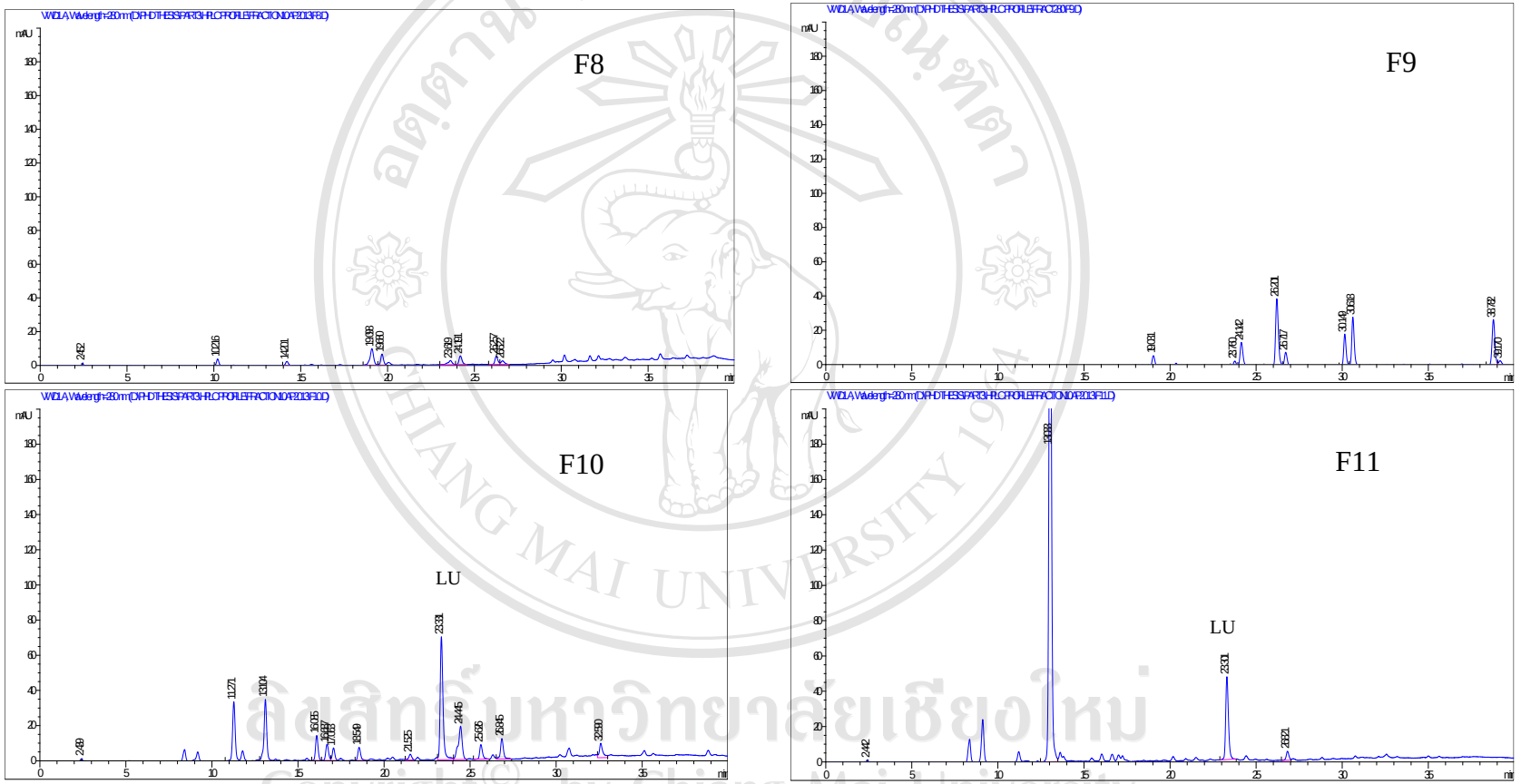

Figure 3.13 (cont.) HPLC chromatograms of the fractions separated on the silica gel 60 column chromatography

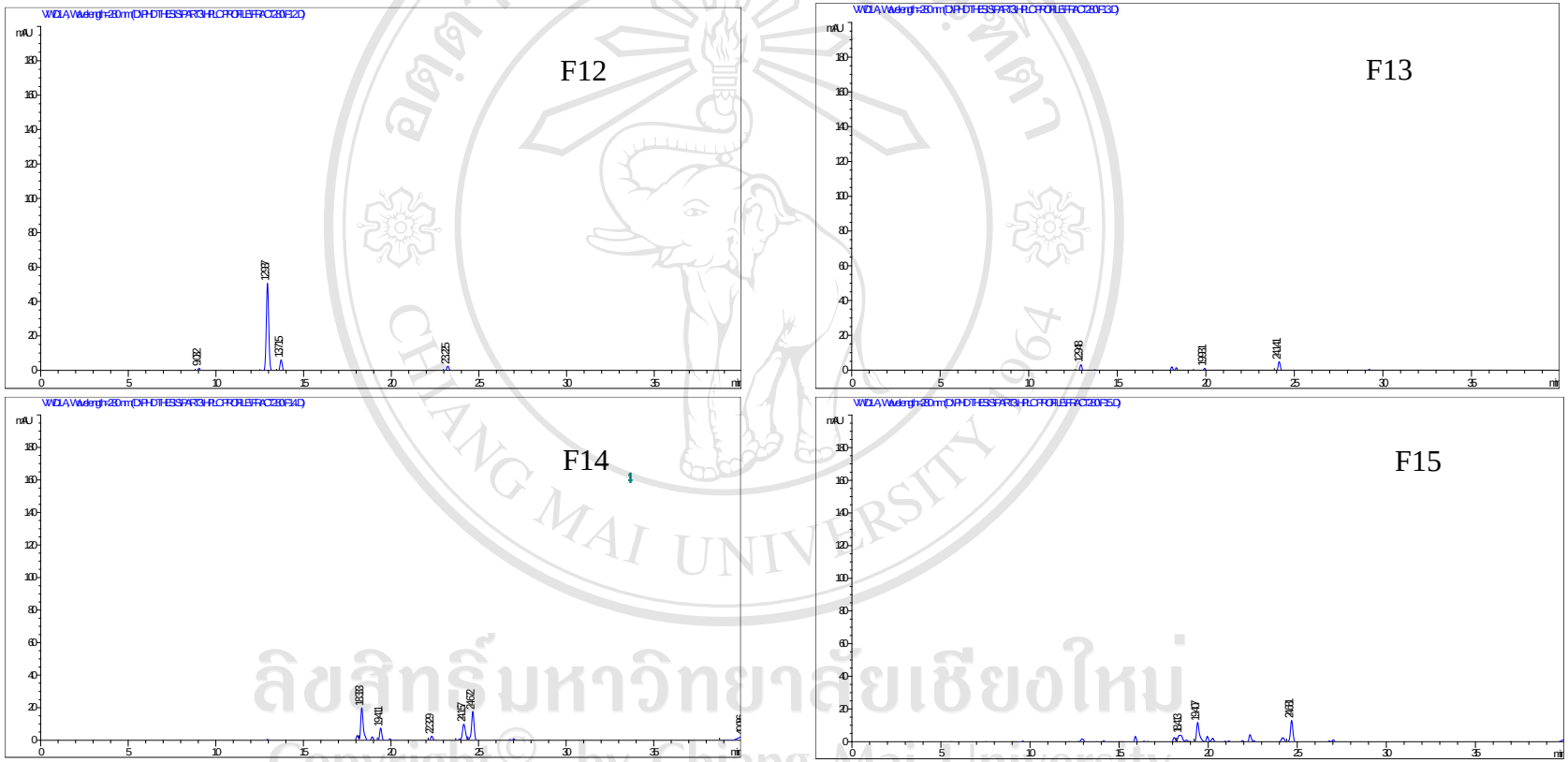

Figure 3.13 (cont.) HPLC chromatograms of the fractions separated on the silica gel 60 column chromatography

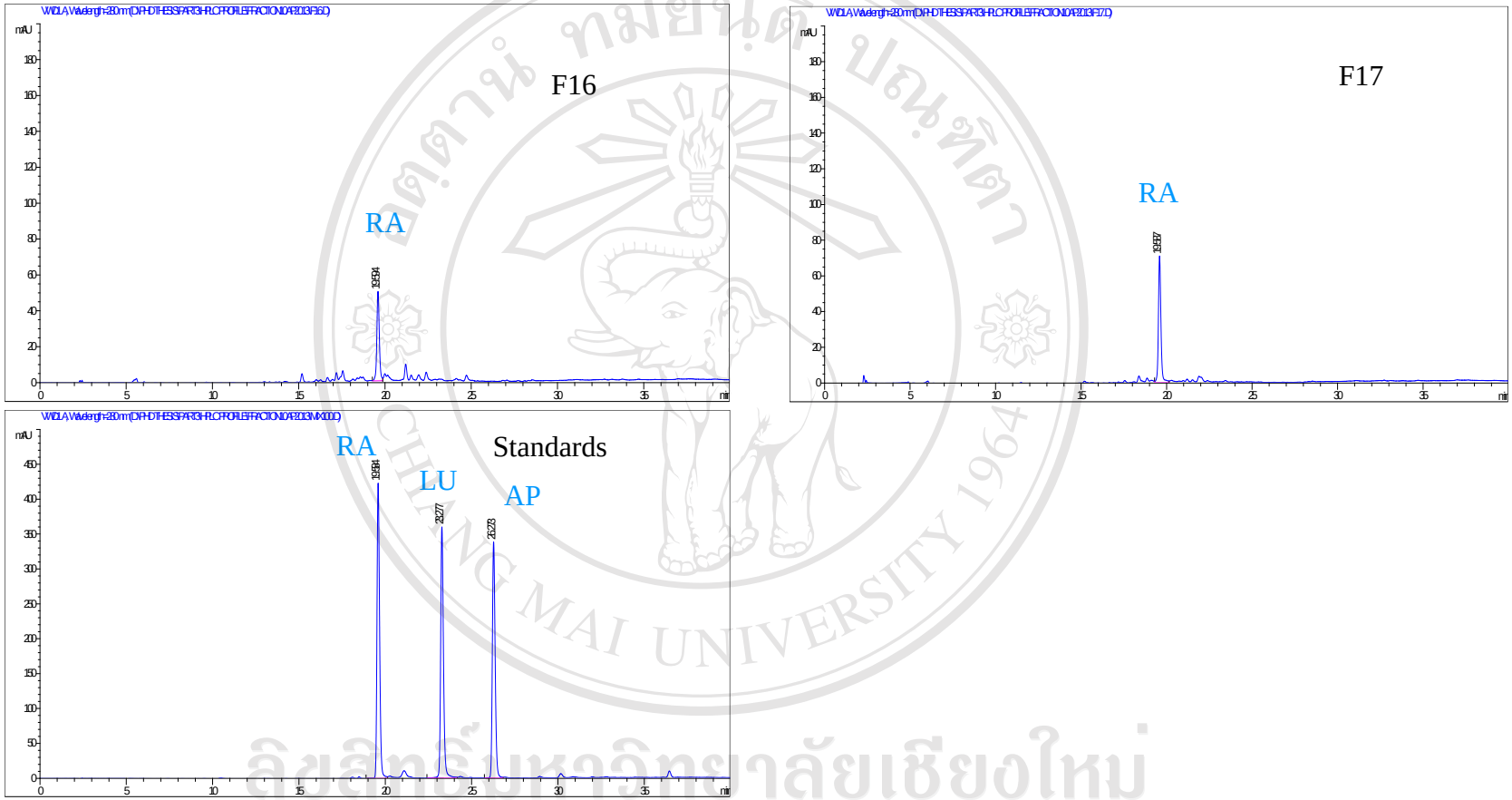

Figure 3.13 (cont.) HPLC chromatograms of the fractions separated on the silica gel 60 column chromatography and of rosmarinic acid (RA), luteolin (LU) and apigenin (AP) standards

3.3.4 Identification of the selected fractions from *Ocimum sanctum* (purple)

3.3.4.1 Gas chromatography / mass spectrometry (GC-MS) analysis of the oil fractions

The separation of the EA fraction from *O. sanctum* (purple) was done to obtain oil fractions (F1-F4). Therefore, these fractions were identified using a Hewlett-Packard 6850 series GC-MS (5% phenyl methyl siloxane, column). The mass spectrum of each constituent was analyzed by comparing them with the NIST05 mass spectral library in which the matching quality was recorded (Table 3.10). The GC-MS chromatogram (Figure 3.13) of fractions F1 and F2, which had a single peak, exhibited the mass spectral pattern of methyl eugenol at 19.87 min (99% similarity), while fraction F3 showed a mass spectral pattern of eugenol as a minor peak, and methyl eugenol as a major peak at 18.27 and 19.83 min, respectively. In addition, fraction F4 revealed a mass spectral pattern of methyl eugenol at 19.87 min (99% similarity) as a major peak and borneol at 11.95 min (99% similarity) as a minor peak.

Table 3.10 Chemical compositions of oil fractions (F1-F4) from *Ocimum sanctum* (purple) identified by GC-MS

Fractions	compounds	t_R (min)	Peak area (%)
F1	Methyl eugenol	19.87	100
F2	Methyl eugenol	19.87	100
F3	Eugenol	18.27	1.92
	Methyl eugenol	19.83	98.08
F4	Borneol	11.95	21.04
	Methyl eugenol	19.87	78.96

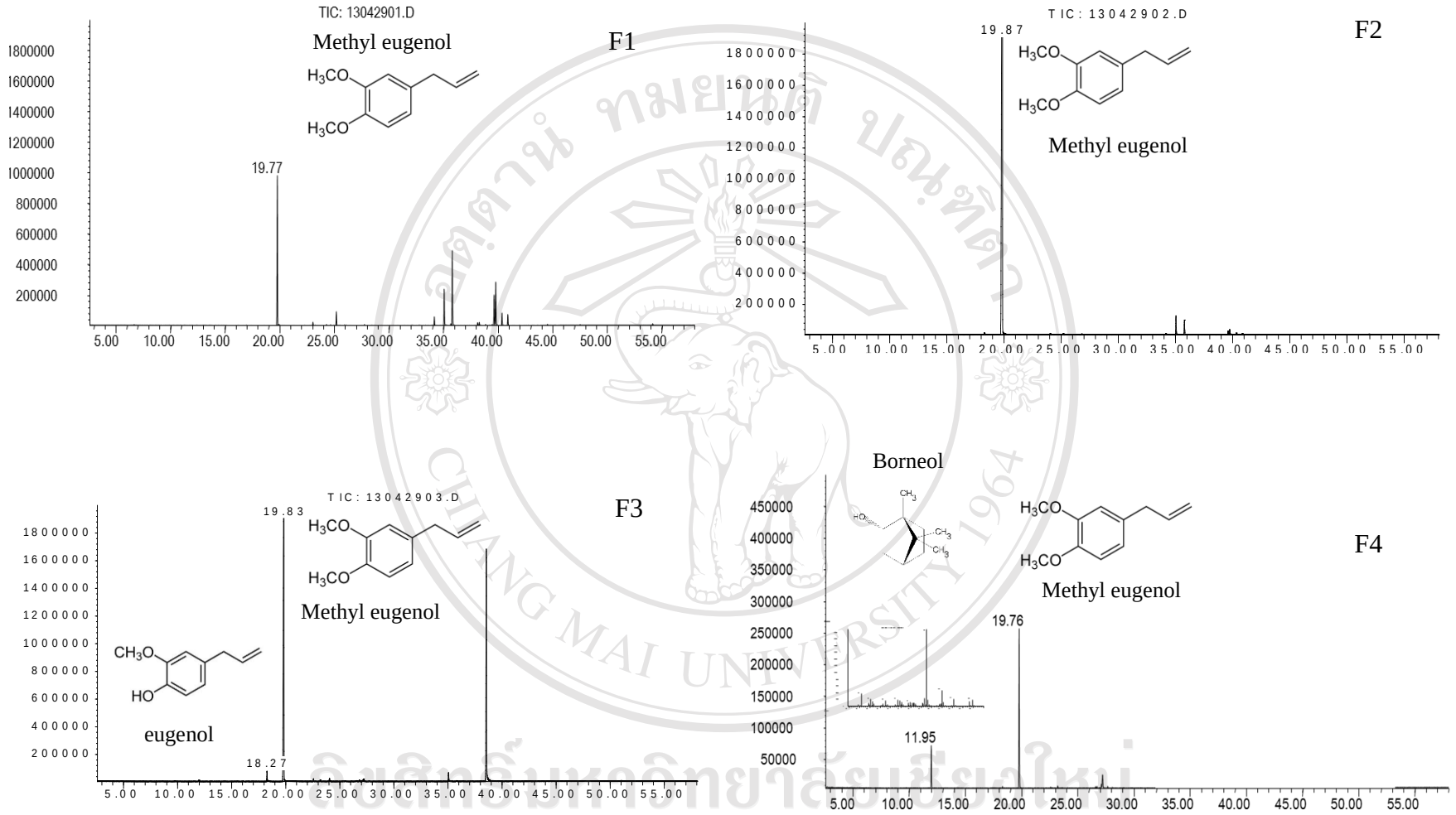

Figure 3.14 GC-MS chromatogram of the oil fractions (F1-F4) of *Ocimum sanctum* (purple). Peak identification: methyl eugenol ($C_{11}H_{14}O_2$), eugenol ($C_{10}H_{12}O_2$) and borneol ($C_{10}H_{18}O$)

3.3.4.2 Liquid chromatography / mass spectrometry (LC-MS) analysis of the fractions (F10 and F16) of *Ocimum sanctum* (purple)

Due to the efficiency in suppressing the AGE formation and α-glucosidase activity of the separated fractions F10 and F16 from *Ocimum sanctum* (purple) (in section 3.3.3), the bioactive compounds in these fractions, particularly the phenolic compounds that might be responsible for AGE inhibition, were identified. The results of the HPLC analysis in Figure 3.13 were confirmed by using LC-MS analysis and comparing the results with the mass spectra of the reference standards. The LC-MS chromatogram of the fraction F10 exhibited the mass spectral at *m/z* 269.1 $[M-H]^-$ and 285.0 $[M-H]^-$, which was similar to the mass spectrum patterns of standard apigenin and luteolin, respectively. Whereas the LC-MS chromatogram of the fraction F16 showed the mass spectral pattern at *m/z* 359.1 $[M-H]^-$. According to a comparison using the mass spectrum (MS) of standards, the peaks in the chromatogram of fraction F10 were identified as rosmarinic acid (Figure 3.15).

3.3.4.3 Liquid chromatography-tendem mass spectrometry (LCMS/MS) analysis of the fractions F1 and F10 of *Ocimum sanctum* (purple)

Based on the results in sections 3.3.2 and 3.3.3, the spectral data of fractions F1 and F10 from *O. sanctum* (purple) was confirmed by LCMS/MS. The HRMS (ESI) spectrum of fractions F1 and F10 revealed a molecular ion peaks of $[M-Na^+]$ and $[M-H^+]$ at m/z 201.0888 and 287.0544 (Figure 3.16-3.17) corresponding to the mass spectral patterns of methyl eugenol and luteolin, respectively. The molecular formula of the structure was obtained from the calculated spectral data for methyl eugenol and luteolin, which were $C_{11}H_{14}O_2Na$ and $C_{15}H_{11}O_6$, respectively.

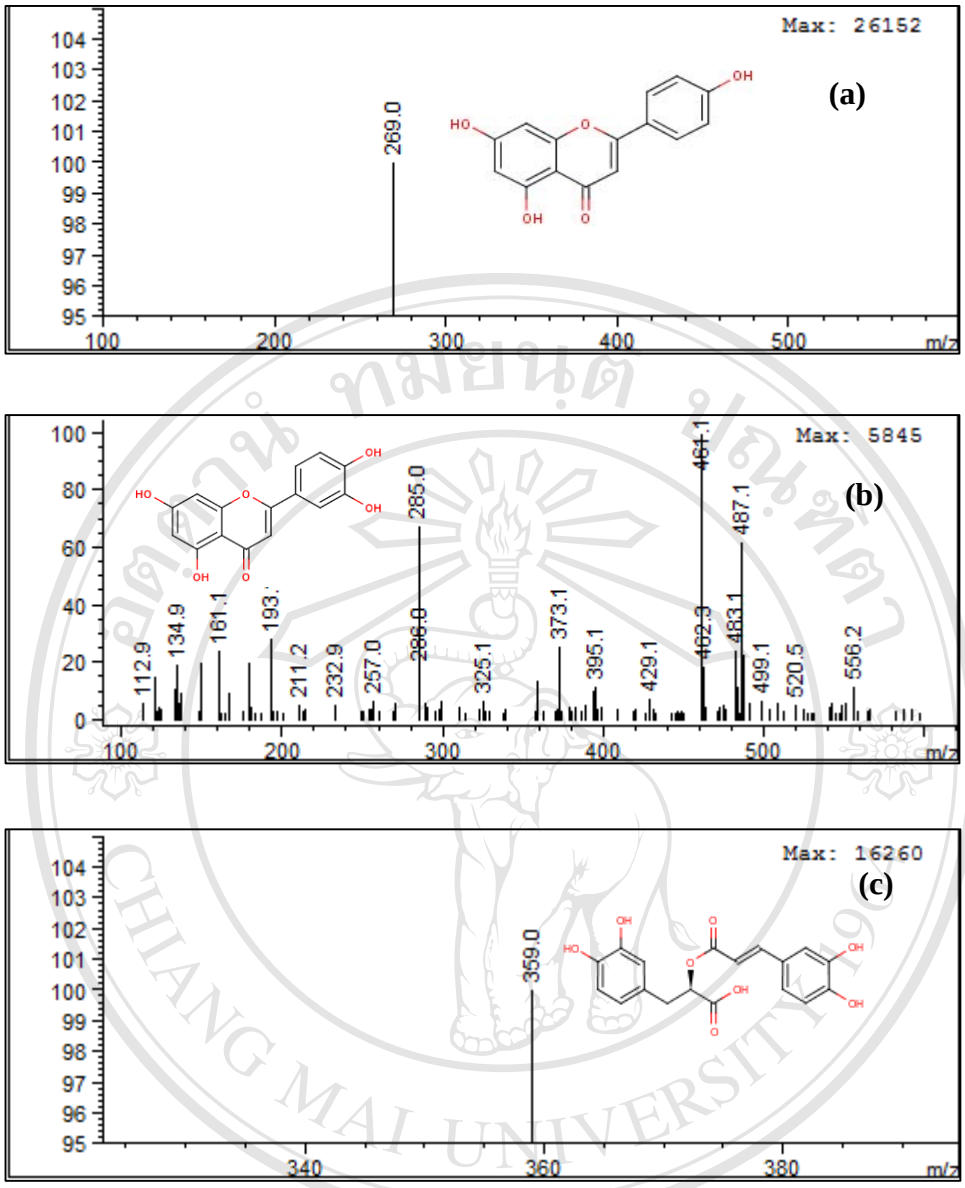

Figure 3.15 LC-MS chromatogram of fractions F10 and F16 separated on silica gel 60 column chromatography of *Ocimum sanctum* (purple), (a) apigenin at *m/z* 269.1 $[M-H]^-$, (b) luteolin at m/z 285.0 $[M-H]^-$ and (c) rosmarinic acid at m/z 359.1$[M-H]^-$

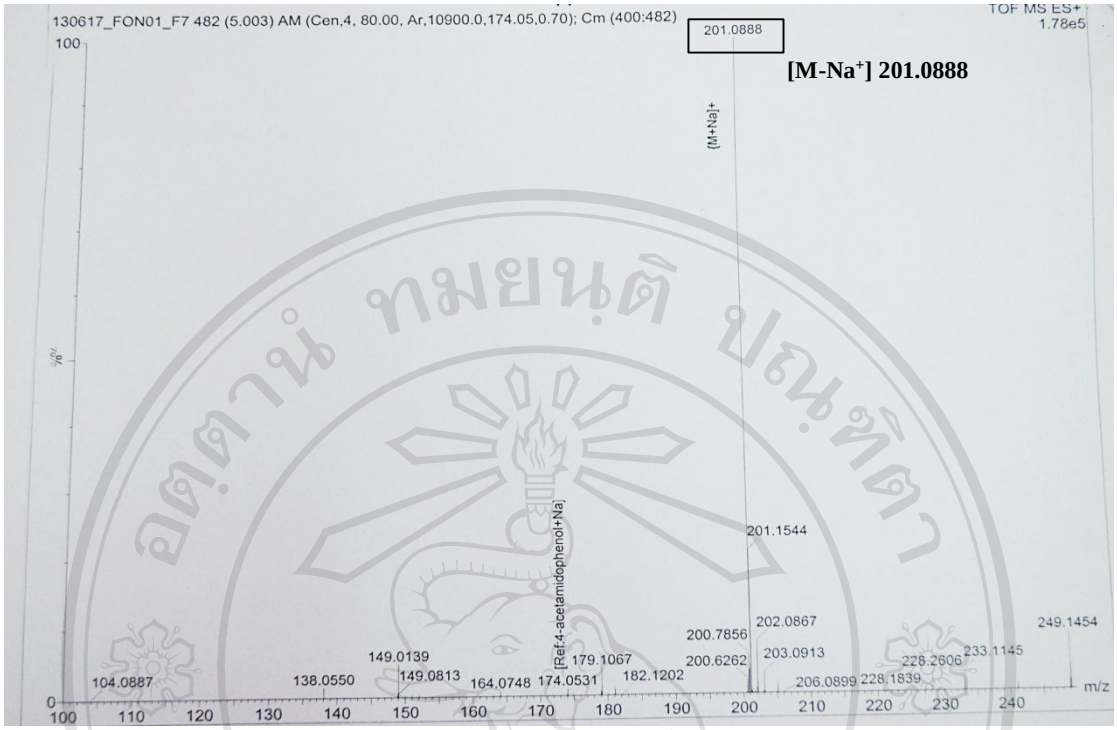

Figure 3.16 HRMS (ESI) spectrum of the separated fraction F1 from *Ocimum sanctum* (purple)

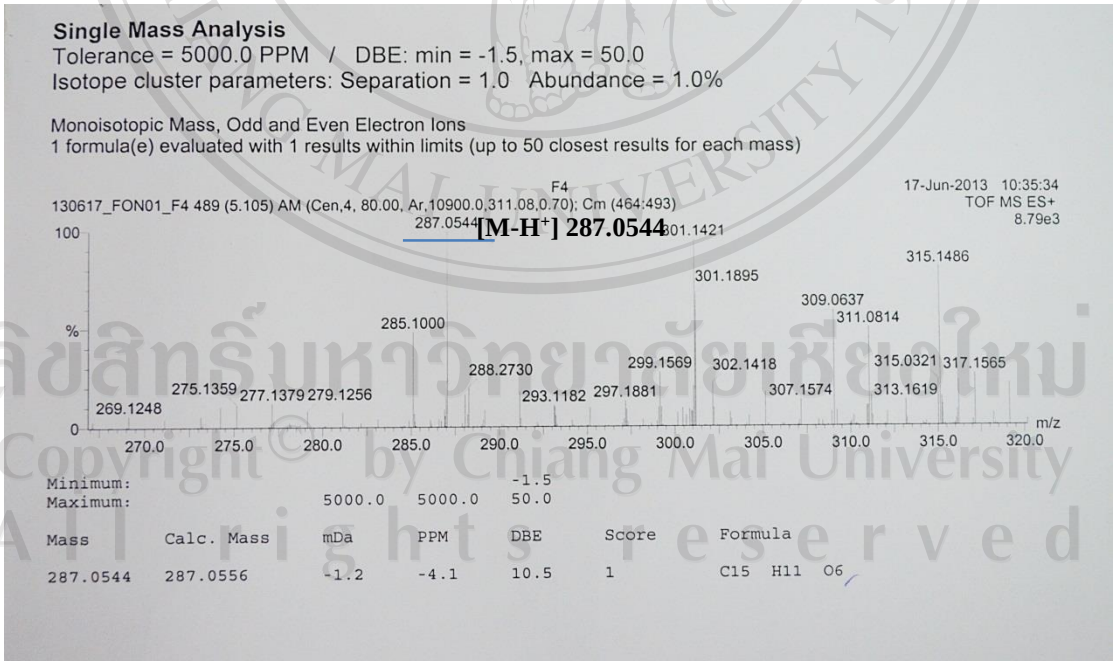

Figure 3.17 HRMS (ESI) spectrum of the separated fraction F10 from *Ocimum sanctum* (purple)

3.3.5 Quantification of the identified phenolic compounds (methyl eugenol, rosmarinic acid, luteolin and apigenin) in *Ocimum sanctum* (purple)

The individual identified phenolic compound in the ethyl acetate and aqueous extract of *O. sanctum* (purple) was quantified using HPLC by the external standard method. The four phenolic compounds were identified as rosmarinic acid, luteolin, apigenin and methyl eugenol (Figure 3.18). The total amounts of rosmarinic acid (RA), methyl eugenol (ME), luteolin (LU) and apigenin (AP) in the EA and aqueous fractions are displayed in Table 3.11. The results showed that the EA fraction contained high amounts of rosmarinic acid (6.49 mg/g extract), followed by methyl eugenol (2.82 mg/g), luteolin (0.97 mg/g extract) and apigenin (0.41 mg/g extract), respectively, while these phenolic compounds were not detected in the aqueous fraction.

Table 3.11 Amounts of rosmarinic acid, luteolin, apigenin and methyl eugenol in the EA and aqueous fractions of *Ocimum sanctum* (purple)

extract	Phenolic compounds (mg/g extract)			
	rosmarinic acid	luteolin	apigenin	methyl eugenol
EA fraction	6.49	0.97	0.41	2.82
% relative	60.7	9.1	3.8	26.4
Aqueous fraction	ND	ND	ND	ND
%relative	-	-	-	-

ND is not detected. EA= ethyl acetate.

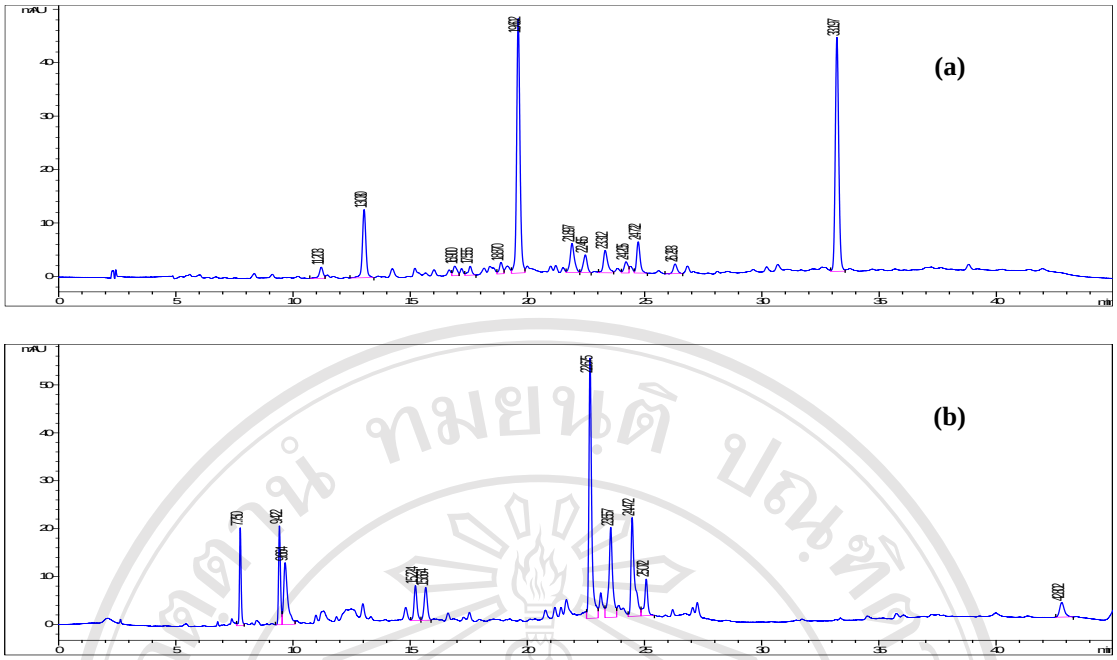

Figure 3.18 HPLC chromatogram of ethyl acetate (EA) and aqueous fractions of *Ocimum sanctum* (purple); (a) ethyl acetate (EA) fraction, (b) aqueous fraction

3.4 Inhibitory effects of phenolic compounds in *Ocimum sanctum* (purple) on α-glucosidase activity and the formation of advanced glycation end-products (AGEs)

3.4.1 Effect of different inducers on the AGE formation in model proteins

The formation of fluorescent AGEs on collagen (1mg/mL), induced by different inducers (D-glucose, D-ribose and MGO) at different concentrations (1, 5 and 10 mM) were monitored for 15 days of incubation at 37°C and were also assessed on histone (1 mg/mL) and BSA (10 mg/mL) models after 7 and 15 days of incubation time. Figure 3.19 shows the intensity of AGE fluorescence on various model proteins induced by different inducers at different concentration. These results could observe that all of inducers (MGO, D-ribose and D-glucose) displayed the potential to produce AGE formation in all model proteins. Especially, MGO and D-ribose could induce the AGE formation faster than D-glucose. The findings indicated that these inducers not only could form AGE formation in extracellular proteins (BSA and collagen), but so also affected in intracellular proteins (histone).

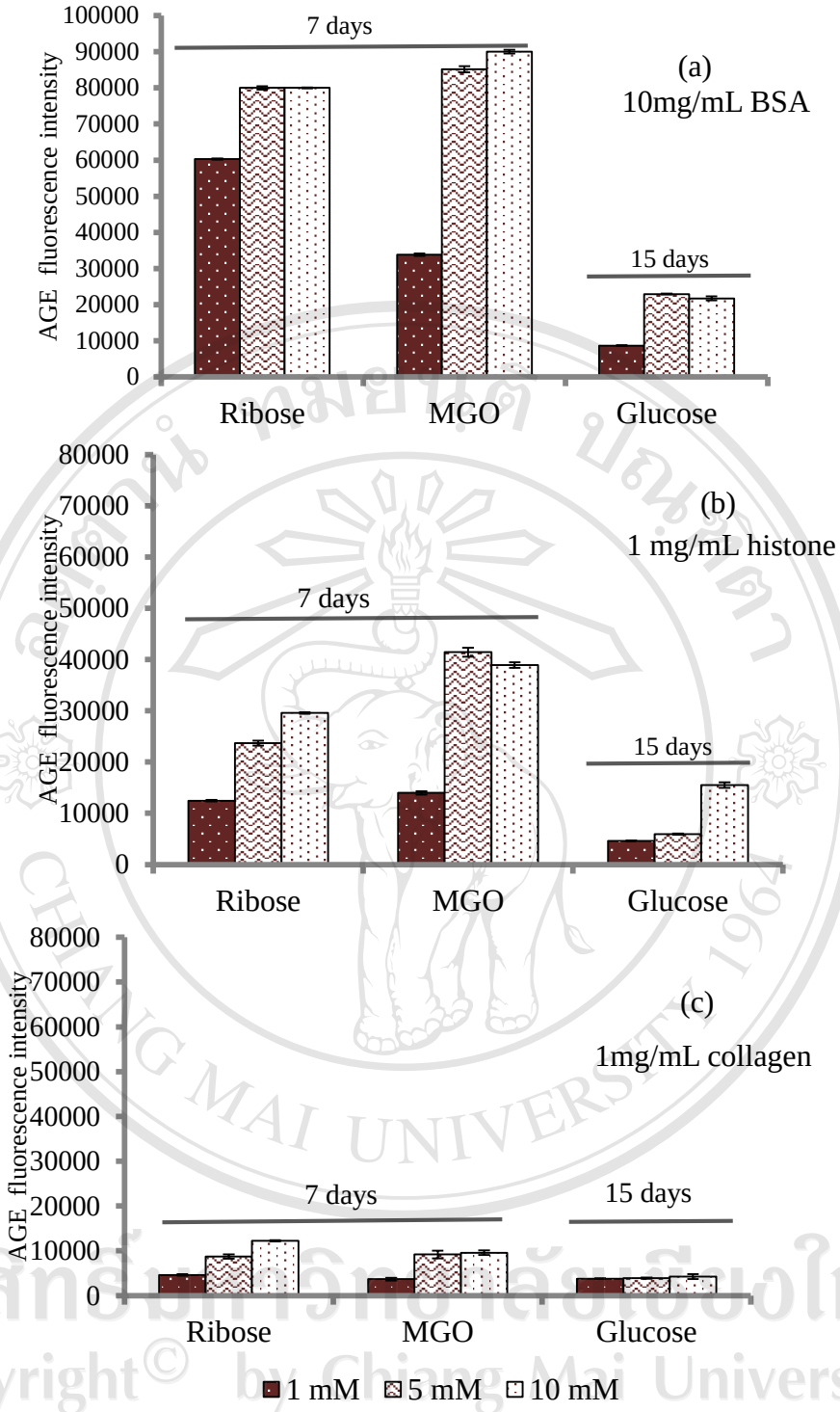

Figure 3.19 AGE fluorescent intensity of various model proteins (BSA, histone and collagen) induced by D-glucose, methylgloxal (MGO) and D-ribose at various concentrations after being incubated for 7 - 15 days at 37°C

3.4.2 Inhibitory effects of *Ocimum sanctum* (purple) fractions on the AGE formation in model proteins (BSA, histone and collagen)

3.4.2.1 Inhibitory effects of *Ocimum sanctum* (purple) on the AGE formation induced by different inducers

It is well understood that the advanced glycation end-products (AGEs) are formed between proteins and by reducing sugars through oxidative and non-oxidative pathways. Therefore, the inhibitory effects of EA and the aqueous fractions from *O. sanctum* (purple) on the glycation of BSA induced by different reducing sugars (glucose, ribose and MGO) were investigated and compared with the selected standard phenolic compounds (luteolin, apigenin, romarinic acid and methyl eugenol). Table 3.12 indicates a strong inhibitory effect of the EA fraction from *O. sanctum* (purple) against the glycation of BSA induced by MGO (IC_{50} value of 0.294 mg/mL), glucose (IC_{50} value of 0.432 mg/mL) and ribose (IC_{50} value of 0.434 mg/mL). However, its aqueous fraction exhibited weak inhibitory effects in 3 different inducer models. These results imply that the active compounds in the EA fraction of *O. sanctum* (purple) displayed a potent suppressing ability on the AGE formation that was not only induced by MGO and ribose, but also by glucose. In the case of the selected phenolic standards including luteolin, apigenin and rosmarinic acid, these standard compounds also demonstrated strong AGE suppressive capabilities induced by glucose (IC_{50} value of 0.006 to 0.2 mg/mL), ribose (IC_{50} value of 0.024 to 0.164 mg/mL) and methylglyoxal (IC_{50} value of 0.016 to 0.104 mg/mL). However, methyl eugenol showed no antiglycation activities with all the different inducers.

Table 3.12 Inhibitory effects of *Ocimum sanctum* (purple) extracts on AGE formation in Bovine serum albumin (BSA) induced by glucose, ribose and methylglyoxal (MGO)

	IC_{50} values (mg/mL)		
Extract	**glucose-BSA**	**ribose-BSA**	**MGO-BSA**
EA extract	0.432 ± 0.0^{a}	0.434 ± 0.0^{b}	0.294 ± 0.0^{b}
aqueous extract	>1	0.825 ± 0.0	>1
	IC_{50} values (mg/mL)		
Standards	**glucose-BSA**	**ribose-BSA**	**MGO-BSA**
Luteolin	0.006 ± 0.0^{a}	0.024 ± 0.0^{c}	0.017 ± 0.0^{b}
Apigenin	0.012 ± 0.0^{a}	0.032 ± 0.0^{b}	0.016 ± 0.0^{a}
rosmarinic acid	>0.2	0.164 ± 0.0^{b}	0.104 ± 0.0^{a}
aminoguanidine(AG)	0.066 ± 0.0^{a}	0.152 ± 0.0^{c}	0.092 ± 0.0^{b}
Methyl eugenol	NI	NI	NI

-Values are expressed as means±SD.

- $^{a\text{-}c}$ means in the row followed by different letters are significantly different ($p<0.05$)

- NI is not inhibition

3.4.2.2 Inhibitory effects of *Ocimum sanctum* (purple) on AGE formation in different model proteins

A) Glycation of histone

Similarly to the BSA model, the EA fraction of *O. sanctum* (purple) was more effective in suppressing AGE formation in the histone-MGO model with an IC_{50} value of 0.290 mg/mL than the aqueous fraction (IC_{50} = 0.809 mg/mL). Whereas, luteolin and apigenin, flavonoid compounds showed stronger AGE formation than the AG standard inhibitor (Figure 3.20).

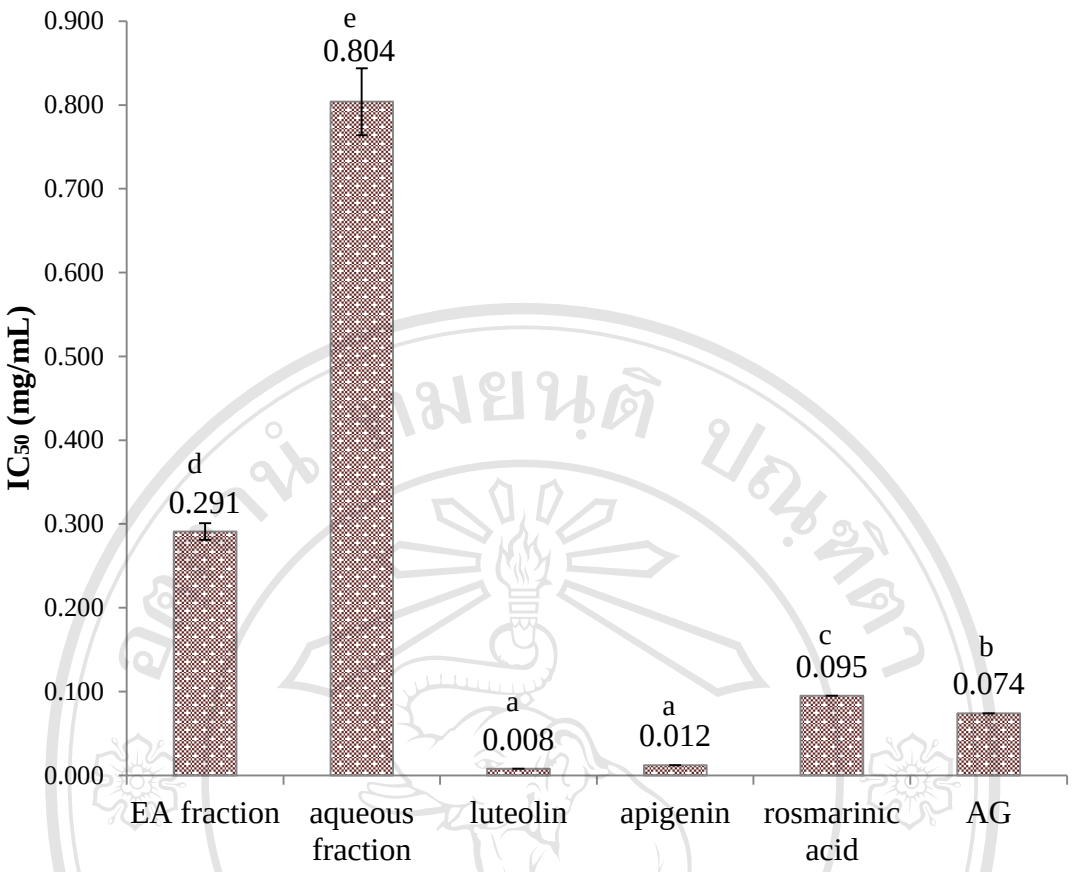

Figure 3.20 Effects of *Ocimum sanctum* (purple) extracts and the standard phenolic compounds on AGE formation in histone (1 mg/mL) induced by 5 mM methylglyoxal (MGO)

B) Glycation of collagen

Collagen is another model protein which has been used to study the inhibitory effects of *O. sanctum* (purple) extracts and its authentic phenolic compounds because the glycation of collagen leads to an initial risk factor of cardiovascular disease, retinopathy and Alzheimer's disease. Collagen (1mg/mL) was incubated with 5 mM MGO with and without the extracts (100 and 200 µg/mL) and standards (10 and 100 µg/mL) for 15 days at 37°C, measuring at an excitation wavelength of 370 nm and an emission wavelength of 440 nm. The results showed that the EA fraction of *O. sanctum* (purple) displayed the more suppressive effect against AGE formation in collagen than the aqueous fraction. Luteolin, apigenin and rosmarinic acid showed stronger AGE formation than the AG standard inhibitor when compared at the same concentration levels (Figure 3.21).

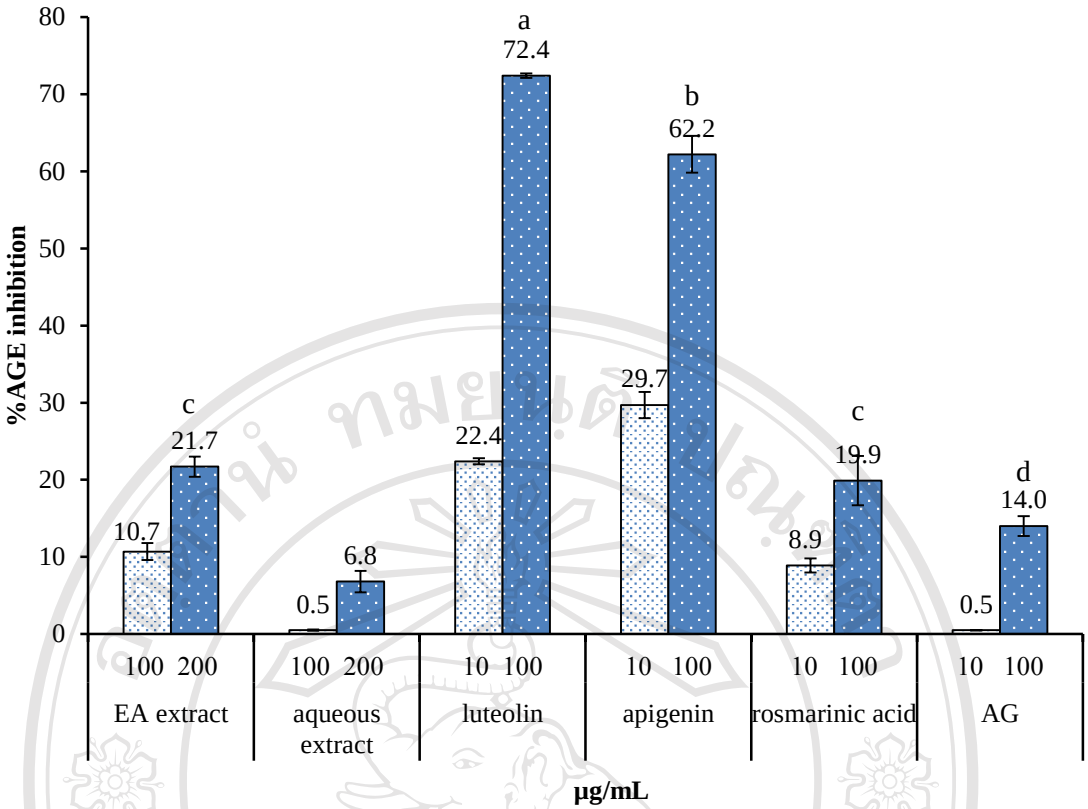

Figure 3.21 Effect of *Ocimum sanctum* (purple) extracts and the standard phenolic compounds on MGO induced collagen-linked fluorescent adduct formation. Collagen (1mg/mL) was incubated with 5 mM MGO with and without of the extracts (100 and 200 µg/mL) and standards (10 and 100 µg/mL) for 15 days at 37°C. AG; aminoguanidine

3.4.3 Determination of the inhibition mode and *Ki* and IC_{50} values of α-glucosidase inhibitory activity of the fractions from *Ocimum sanctum* (purple)

α-glucosidase is a key enzyme involved in sugar metabolism. The α-glucosidase inhibition is considered to be one of several therapeutic approaches used to decrease hyperglycemia in diabetic patients. In this study, the inhibitory effects of the EA and aqueous fractions of *O. sanctum* (purple) on α-glucosidase were also determined by comparing them with the standard phenolic compounds, from which the dissociation constant (*Ki*) and the IC_{50} value were also determined. *p*NPG was used as a

substrate and used to measure the released *p*-nitrophenol at 405 nm. Table 3.13 presents the results of *Ki* and IC_{50} values for the α-glucosidase inhibitory activity of the EA and aqueous fractions from *O. sanctum* (purple) compared with the selected standard phenolic compounds and acarbose. The EA fraction from *O. sanctum* (purple) showed the strongest inhibitory activity with IC_{50} and *Ki* values of 1.72 and 1.02 mg/mL, respectively, while its aqueous fraction revealed weak levels of inhibition (IC_{50} and *Ki* values of 8.02 and 3.82 mg/mL, respectively). However, the EA fraction was less effective than acarbose, which is the synthetic standard inhibitor (IC_{50} and *Ki* values of 0.19 and 0.10 mg/mL, respectively). In the case of the selected phenolic compounds, luteolin and apigenin showed strong inhibitory activity in terms of their IC_{50} values (0.14 and 0.24 mg/mL, respectively) and their *K*i values (0.09 and 0.14 mg/mL, respectively). On the other hand, rosmarinic acid and methyl eugenol showed a weak level of inhibition against the α-glucosidase with IC_{50} values of 2.13 and 2.80 mg/mL, respectively.

Moreover, the types of α-glucosidase inhibition of the EA and aqueous fractions of *O. sanctum* (purple) were also determined by comparing them with the selected standard phenolic compounds. The Lineweaver-Burk plot of their inhibition is displayed in Figure 3.22. Both the EA and aqueous fractions of *O. sanctum* (purple) generated straight lines which had different intersections on the *x*-axis, indicating that their α-glucosidase inhibition were of the mixed non-competitive type. The mixed non-competitive inhibition of these fractions indicated that their inhibition resulted from the binding of both the free enzymes or took place in the enzyme-substrate complex. In the case of the standard phenolic compounds, both luteolin and apigenin also showed their inhibition types as being of the mixed non-competitive inhibitor type (Figure 3.23). While, rosmarinic acid and methyl eugenol displayed the patterns of competitive inhibition due to their intersections on the *y*-axis at the same point (Figure 3.24), indicating that both of these compounds compete with the substrate in binding to the active site of the enzyme.

Table 3.13 Results of calculated *Ki* and IC_{50} values of α-glucosidase inhibitory activity, type of inhibition and total content of the EA and aqueous fractions of *Ocimum sanctum* (purple) compared with the standard phenolic compounds

	α-glucosidase inhibition		
Extract	K_i **(mg/mL)**	IC_{50}**(mg/mL)**	**Type of inhibition**
EA extract	1.02	1.72	mixed
aqueous extract	3.82	8.02	mixed
Standards	K_i **(mg/mL)**	IC_{50}**(mg/mL)**	**Type of inhibition**
luteolin	0.09	0.14	mixed
apigenin	0.14	0.24	mixed
rosmarinic acid	1.21	2.13	competitive
methyl eugenol	2.04	2.80	competitive
acarbose	0.10	0.19	mixed

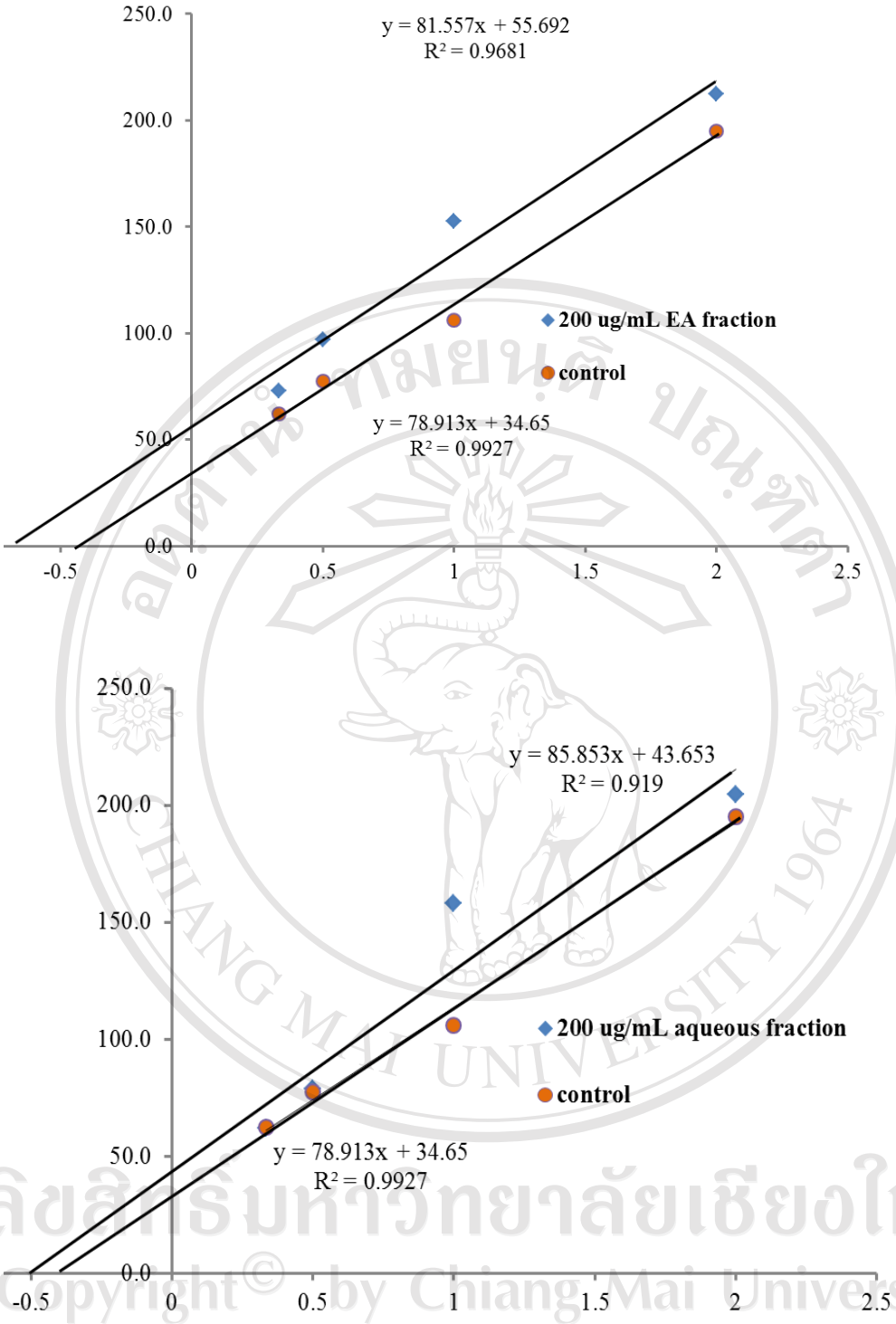

Figure 3.22 The Linweaver-Burk plots of the EA (a) and aqueous (b) fractions of *Ocimum sanctum* (purple) at different concentrations (0 and 200 µg/mL)

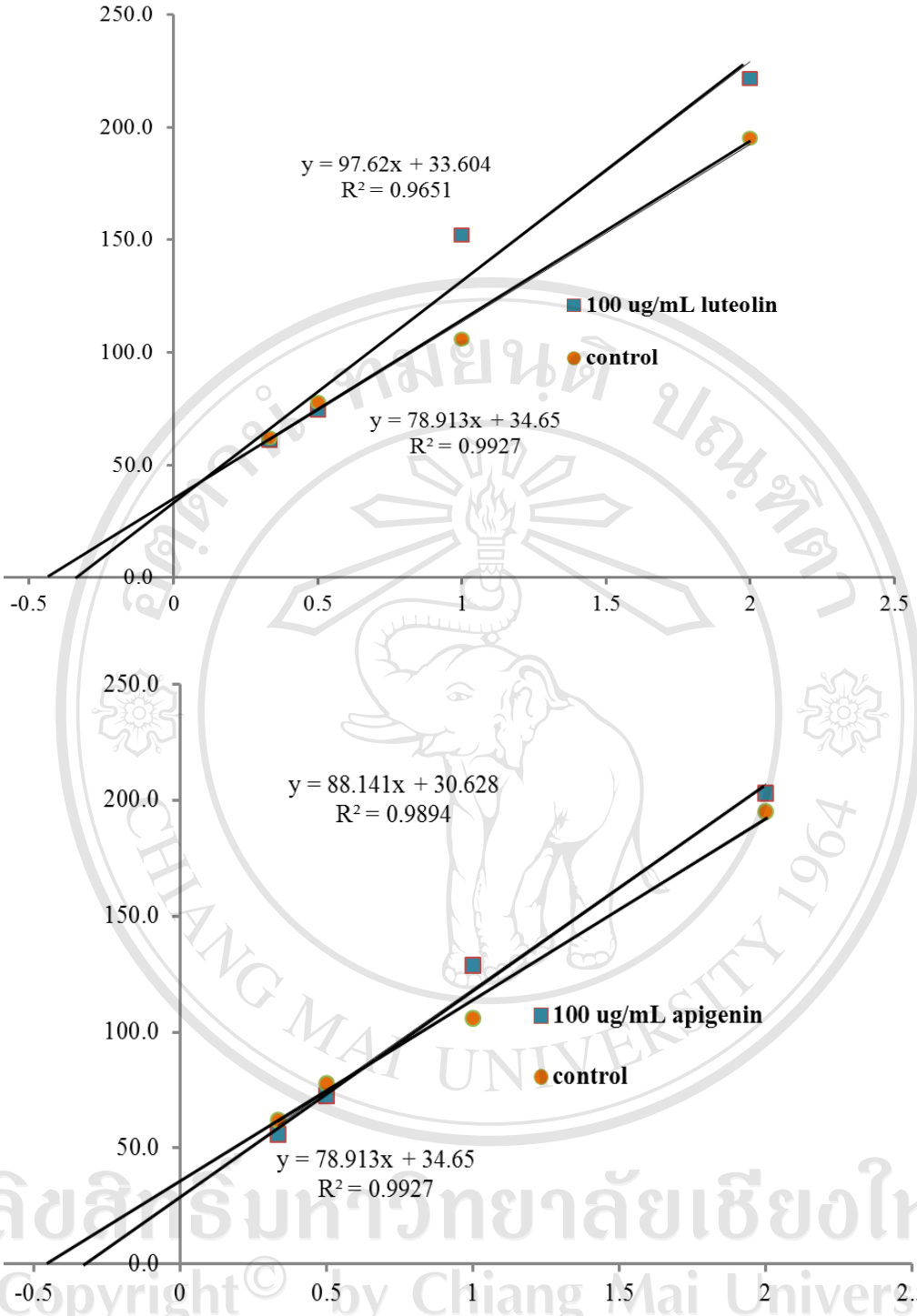

Figure 3.23 The Linweaver-Burk plots of luteolin and apigenin (at concentration of 0 and 100 µg/mL), respectively

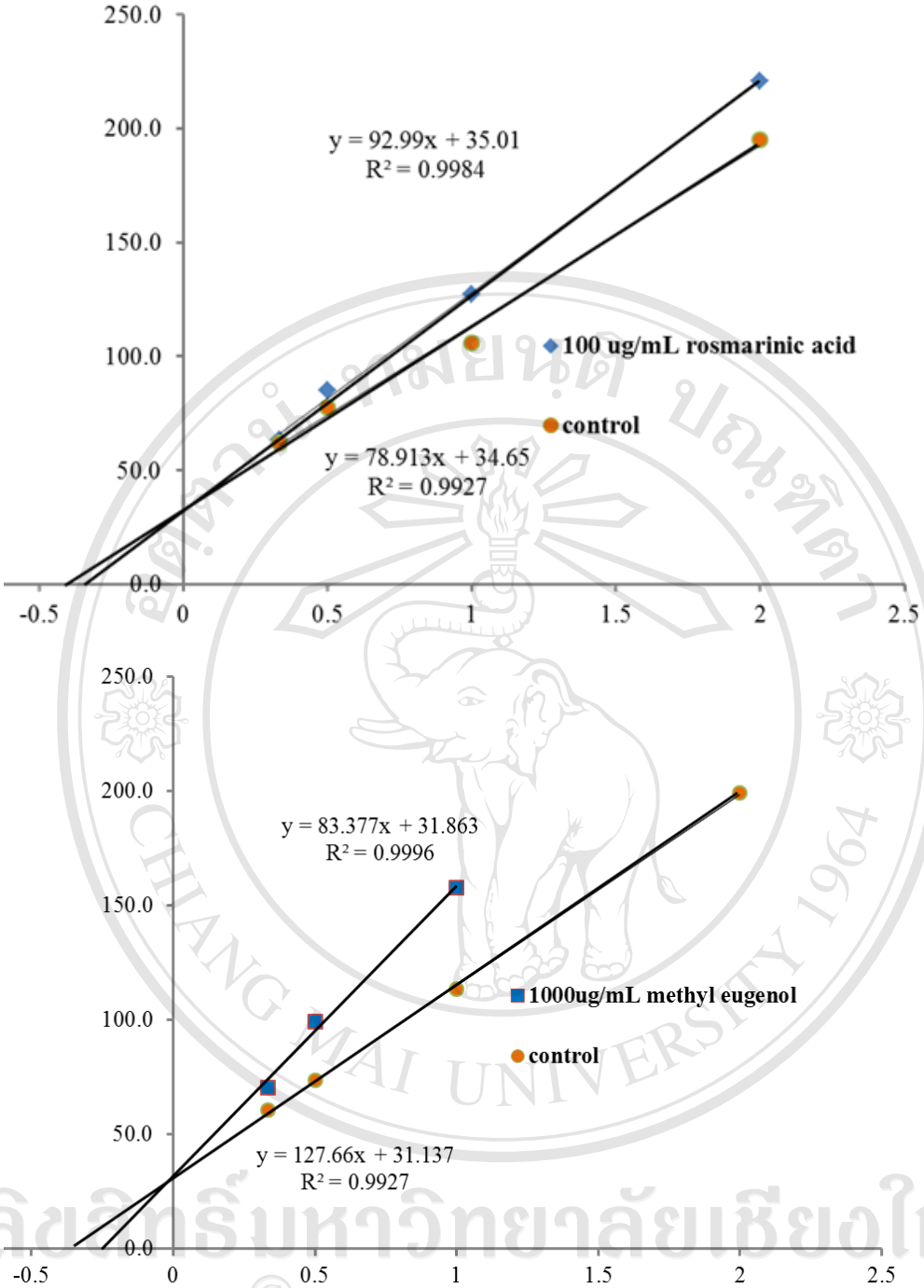

Figure 3.24 The Linweaver-Burk plots of rosmarinic acid (at 0 and 100 µg/mL) and methyl eugenol (at concentration of 0 and 1 mg/mL), respectively

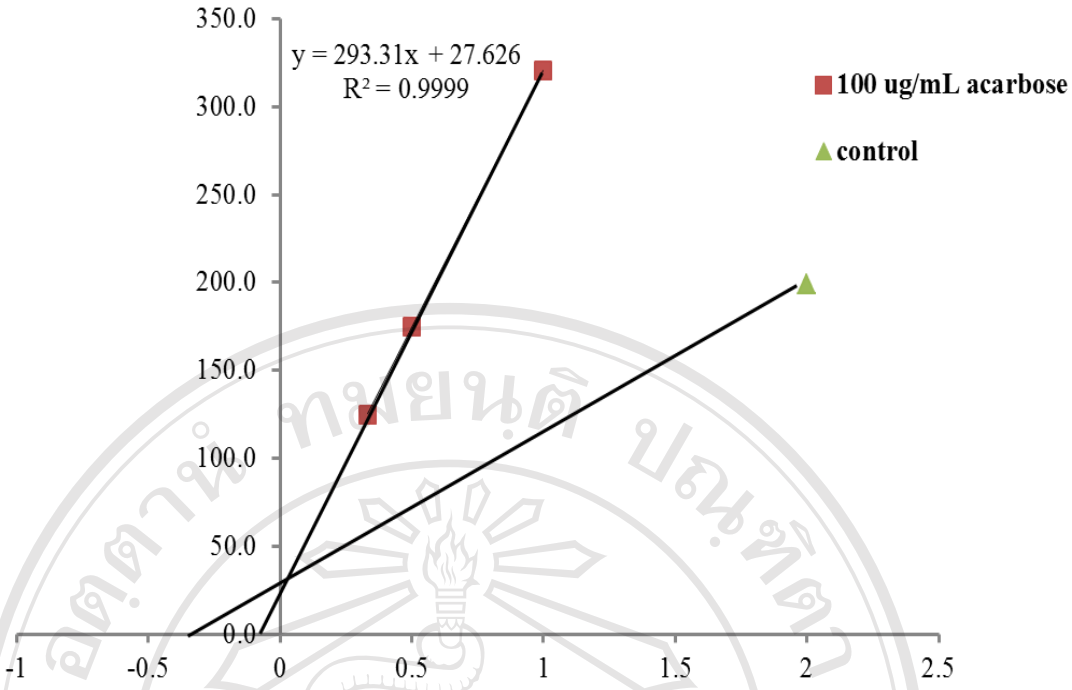

Figure 3.25 The Linweaver-Burk plots of acarbose (at 0 and 100 µg/mL)